Volume 19 | Number 15 | 7 August 2017 | Pages 3431–3680

Green Chemistry

Cutting-edge research for a greener sustainable future

rsc.li/greenchem

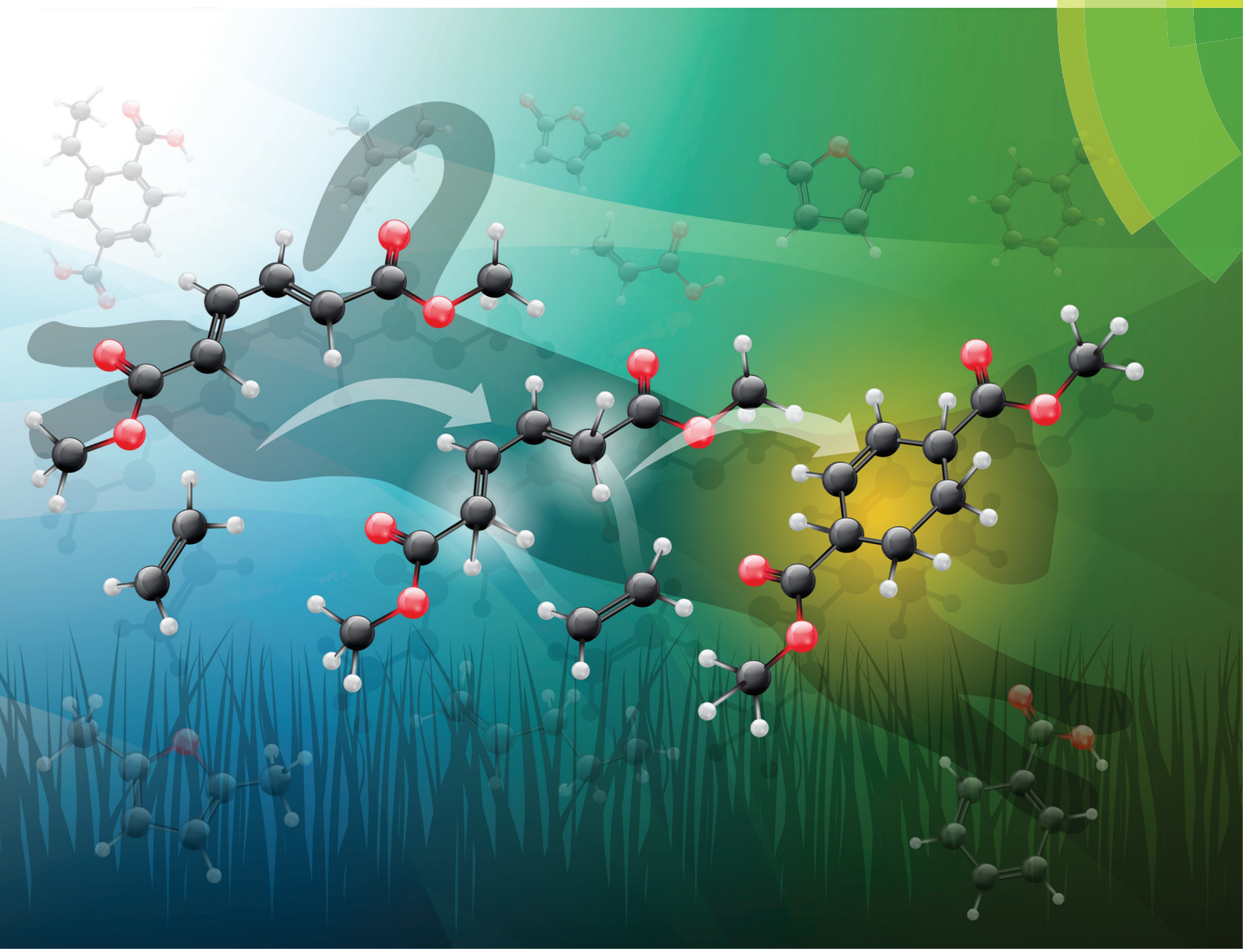

ISSN 1463-9262

ROYAL SOCIETY OF CHEMISTRY

TUTORIAL REVIEW

Derek R. Vardon *et al.*

Heterogeneous Diels–Alder catalysis for biomass-derived aromatic compounds

Green Chemistry

TUTORIAL REVIEW

View Article Online
View Journal | View Issue

Cite this: *Green Chem.*, 2017, **19**, 3468

Heterogeneous Diels–Alder catalysis for biomass-derived aromatic compounds

Amy E. Settle,[a,b] Laura Berstis,[a] Nicholas A. Rorrer,[a] Yuriy Roman-Leshkóv,[c] Gregg T. Beckham,[a] Ryan M. Richards[a,b] and Derek R. Vardon*[a]

In this tutorial review, we provide an overview of heterogeneous Diels–Alder catalysis for the production of lignocellulosic biomass-derived aromatic compounds. Diels–Alder reactions afford an extremely selective and efficient route for carbon–carbon cycloadditions to produce intermediates that can readily undergo subsequent dehydration or dehydrogenation reactions for aromatization. As a result, catalysis of Diels–Alder reactions with biomass-derived dienes and dienophiles has seen a growth of interest in recent years; however, significant opportunities remain to (i) tailor heterogeneous catalyst materials for tandem Diels–Alder and aromatization reactions, and (ii) utilize biomass-derived dienes and dienophiles to access both conventional and novel aromatic monomers. As such, this review discusses the mechanistic aspects of Diels–Alder reactions from both an experimental and computational perspective, as well as the synergy of Brønsted–Lewis acid catalysts to facilitate tandem Diels–Alder and aromatization reactions. Heterogeneous catalyst design strategies for Diels–Alder reactions are reviewed for two exemplary solid acid catalysts, zeolites and polyoxometalates, and recent efforts for targeting direct replacement aromatic monomers from biomass are summarized. Lastly, we point out important research directions for progressing Diels–Alder catalysis to target novel, aromatic monomers with chemical functionality that enables new properties compared to monomers that are readily accessible from petroleum.

Received 31st March 2017,
Accepted 17th May 2017

DOI: 10.1039/c7gc00992e

rsc.li/greenchem

[a]*National Bioenergy Center, National Renewable Energy Laboratory, Golden, CO 80401, USA. E-mail: Derek.Vardon@NREL.gov*
[b]*Department of Chemistry, Colorado School of Mines, Golden, CO 80401, USA*
[c]*Department of Chemical Engineering, Massachusetts Institute of Technology, Cambridge, MA 02139, USA*

Introduction

Growing awareness of environmental concerns and the economic volatility of petroleum products has led to increased interest in the use of biomass-derived sustainable alternatives.

Amy E. Settle

Amy Settle received her B.S. with honors in Chemistry from Colorado Mesa University in 2015, where she conducted research with Professor David R. Weinberg. Post graduation, she worked at the National Renewable Energy Laboratory under the guidance of Dr Derek R. Vardon. She is currently a Ph.D. student in Applied Chemistry at Colorado School of Mines under the supervision of Professor Ryan M. Richards and Dr Vardon. Her research focuses on heterogeneous catalyst design, application, and characterization for biomass upgrading to commodity chemicals.

Derek R. Vardon

Derek Vardon is a Staff Research Engineer at the National Renewable Energy Laboratory (NREL). His research interests include applied catalysis, biomass conversion to fuels and chemicals, hybrid biological and chemo-catalytic processing, and advanced catalyst material synthesis and characterization. Since 2013, he has worked in the National Bioenergy Center at NREL. He received his B.S. (2010), M.S. (2012), and Ph.D. (2015) in Environmental Engineering from the University of Illinois at Urbana-Champaign. Prior to entering college, he served 6 years in the U.S. Navy as a nuclear electrician's mate.

Of note, global consumption of commodity aromatic monomers surpasses 140 million metric tons annually, and the market sizes continue to grow at rates between 2–6% annually.[4,33,40] These aromatic monomers include the hydrocarbons benzene, toluene, and xylenes, commonly referred to as BTX, as well as oxygenated derivatives thereof, including benzoic acid, phthalic anhydride, and terephthalic acid. These aromatic monomers have extensive commercial applications for polymers, solvents, plasticizers, and adhesives. A prominent example is polyethylene terephthalate (PET), which is the most widely produced polyester, primarily used for the synthesis of plastic bottles and textile fibers on the scale of over three million metric tons annually in North America alone.[1] Consequently, there has been an increase in research efforts directed toward production of biomass-derived aromatic compounds.[2–4]

Multiple approaches have been investigated for the production of "direct replacement" aromatic monomers (*i.e.*, structurally-identical substitutes for petroleum-derived monomers) from biomass, including thermochemical, biological, and chemocatalytic processing.[5–8] Thermochemical conversion is typically applied to whole biomass or residual lignin fractions[9,10] *via* fast pyrolysis, catalytic fast pyrolysis, or gasification. During fast pyrolysis, biomass is heated to temperatures typically within a range of 400–600 °C at residence times generally <5 s in the absence of oxygen to thermally degrade biomass and generate vapors that are condensed into a complex organic phase referred to as bio-oil.[11] Bio-oils can contain >300 compounds with significant oxygen content (*ca.* 40%).[12] If targeting hydrocarbon aromatics, oxygen content must be reduced *via* catalytic hydrotreating or cracking reactions.[13–15] Although selectively targeting aromatics can be challenging, ongoing efforts to commercialize bio-oil upgrading have been recently reviewed.[15] Alternatively, catalytic fast pyrolysis involves integrating catalysts with the feedstock during pyrolysis prior to condensation, which has the benefit of removing reactive intermediates in the vapor phase, simplifying unit operations and increasing target aromatic monomer yields.[16,17] Commercialization of catalytic fast pyrolysis for BTX production is currently being pursued at the pilot scale.[18,19] Lastly, biomass gasification occurs at higher temperatures (>750 °C) in the presence of air or steam to produce syngas (*i.e.*, CO and H_2) as the target intermediate.[20] Syngas can undergo subsequent catalytic transformations, such as syngas-to-alcohols followed by alcohol-to-aromatics,[4] or Fischer–Tropsch synthesis followed by hydrocracking,[21] with ongoing commercialization efforts recently reviewed.[22]

As an alternative to thermochemical processing, significant efforts have also focused on selective, low-temperature deconstruction of lignocellulosic biomass to facilitate downstream biological and chemocatalytic processing.[23–31] The most commercially relevant efforts to date involve ethanol production from lignocellulosic sugars. Currently, major commercialization efforts focus on catalytic dehydration of ethanol and oligomerization to BTX.[32–34] Longer chain alcohols, such as isobutanol, can also be produced biologically from lignocellulosic sugars.[35,36] The commercial potential of isobutanol dehydration and oligomerization to *p*-xylene is currently being pursued.[2,37,38] As a solely catalytic route, lignocellulosic sugars can undergo aqueous phase reforming and hydrodeoxygenation to BTX that proceeds *via* hydrogenation, condensation, alkylation, and dehydration reactions. This technology is undergoing commercialization and has the valuable capability to handle mixed C_5 and C_6 lignocellulosic sugar streams.[2,39–41] However, with several of the aforementioned approaches, selectivity to single aromatic monomers presents a challenge because the product stream is a complex mixture of linear, cyclic, and aromatic intermediates.

To address the limitations of aromatic monomer selectivity and feedstock atom efficiency, Diels–Alder cycloadditions have recently emerged as a prominent route to couple biomass-derived chemical intermediates. This is not only due to the immense number of accessible biomass-derived Diels–Alder addends, particularly furans and furan derivatives, but also because Diels–Alder reactions offer a robust route for synthesis of cyclic products. The coupling of a conjugated diene and a dieneophile *via* Diels–Alder cycloaddition produces a six-membered ring that exhibits 100% atom economy. Following Diels–Alder addition, subsequent dehydration or dehydrogenation reactions can generate aromaticity, with both reactions capable of being promoted in tandem over a single heterogeneous catalyst.[42–46] Advancements in metabolic engineering and tailored chemocatalysts are greatly expanding the number of biomass-derived intermediates that can be used for Diels–Alder coupling reactions, which may allow for the production of direct replacement commodity aromatics, as well as new aromatic monomers with diverse chemical functionality – henceforth referred to as "functional alternative" monomers (Scheme 1). These functional alternative monomers may allow for new market applications that cannot be readily addressed by petroleum due to the large number and variety of functional groups present within native biomass, which may alter thermal and mechanical properties of resultant polymeric materials.[31,47–49] While Diels–Alder cycloadditions have historical precedence for applications in pharmacology, agrochemicals, flavors, and fragrances,[50] their capacity for biomass upgrading is just now being realized.

To address the growing field of biomass-derived commodities, this review considers heterogeneous catalysis of Diels–Alder cycloadditions for producing both direct replacement and functional alternative aromatic monomers from lignocellulosic biomass. Mechanistic details are examined for controlling the rate and selectivity of Diels–Alder cycloadditions, with an emphasis on Brønsted–Lewis acid catalysis for tandem reactions and heterogeneous bifunctional catalyst design. Recent efforts are then reviewed for the Diels–Alder production of commodity hydrocarbon and oxygenated aromatic monomers. Illustrative routes for diene and dienophile production from biomass are considered, as well as yields, catalytic materials, and key considerations for converting complex biomass streams into direct replacement aromatics. Lastly, important future research directions are identified for targeting new functional alternative monomers *via* Diels–Alder chemistry.

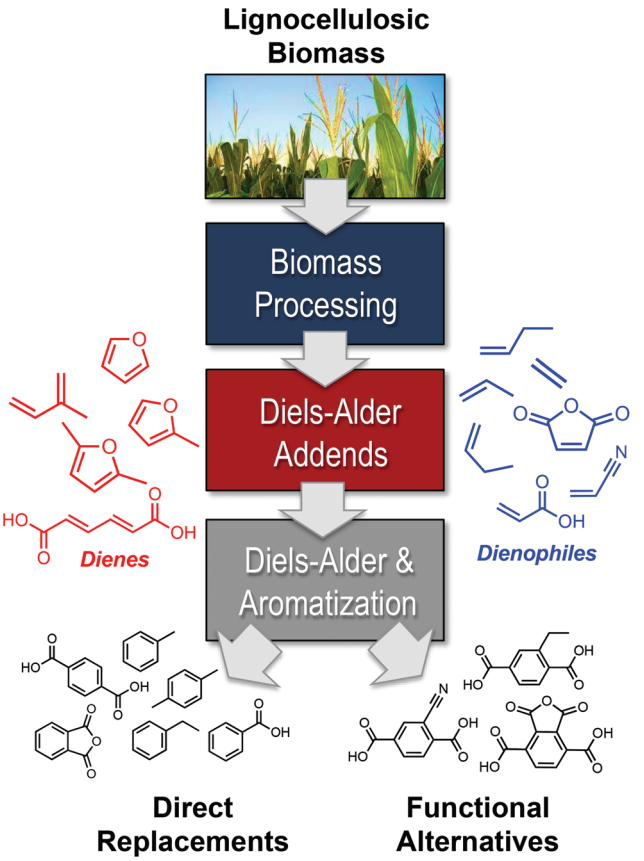

Scheme 1 Lignocellulosic biomass conversion *via* Diels–Alder cycloaddition to produce direct replacement and functional alternative aromatic monomers.

Diels–Alder catalysis

Mechanistic overview

Diels–Alder cycloadditions involve the atom efficient coupling of a diene and dienophile (the "addends") in the preparation of a six-membered ring (the "cycloadduct"), as shown in Fig. 1A. Following the Diels–Alder addition, subsequent dehydration or dehydrogenation reactions can generate aromaticity in the product, as shown in Fig. 1B. Although, in many cases, Diels–Alder reactions alone can be thermally driven to completion, the application of catalysts can greatly enhance reactivity, reduce process severity, mitigate unwanted side reactions, and enable tandem cycloaddition and aromatization reactions over a single catalyst.

At the heart of Diels–Alder cycloadditions is the formation of two σ-bonds between a diene and dienophile at the expense of two π-bonds. It has been hypothesized that these cycloadditions may occur in a concerted one-step mechanism,[51,52] or *via* a two-step reaction in which each new σ-bond is formed in successive steps passing through transition states that involve a biradical intermediate.[53] While the general consensus is that the concerted mechanism dominates, there has been literature to support the multi-step mechanism as well. Spin state-

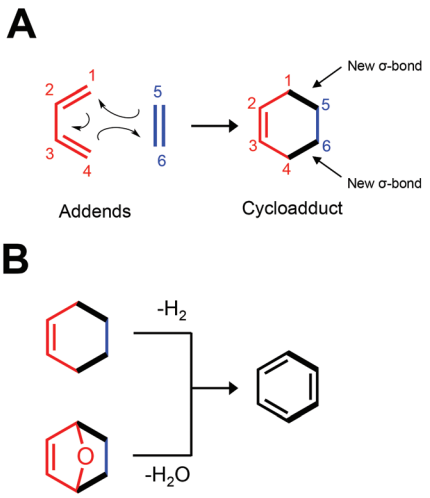

Fig. 1 Diels–Alder cycloaddition of common addends illustrating the formation of two new σ-bonds in the cycloadduct (A). Subsequent dehydrative or dehydrogenative aromatization of two exemplary cycloadducts (B).

corrected density functional theory (DFT) calculations have shown that the difference in free energy of the two-step reaction pathway is a mere 2.3–7.7 kcal mol^{-1} higher than the concerted mechanism in the archetypal Diels–Alder reaction between butadiene and ethylene.[54]

In Diels–Alder reactions, new bond formation occurs through interactions between the highest occupied molecular orbital (HOMO) and lowest unoccupied molecular orbital (LUMO) of the addends (Fig. 2). A normal electron demand (NED) reaction involves the interaction of the HOMO of the diene and the LUMO of the dienophile (Fig. 2, left). Accordingly, the inverse electron demand (IED) reaction involves the HOMO of the dienophile interacting with the LUMO of the diene (Fig. 2, right). The type of electron demand that occurs during a reaction is based largely upon diene and dienophile species and the presence of electron withdrawing or electron donating groups on either. For example, electron-withdrawing groups on the dienophile, such as the carboxylate group of acrylic acid, will expedite NED reactions because of the lowered LUMO energy. Furthermore, catalysts can coordi-

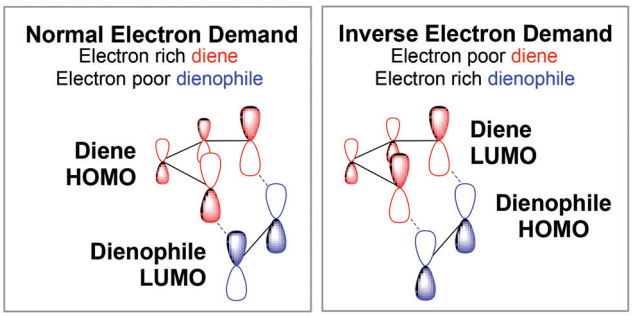

Fig. 2 Representative HOMO–LUMO interactions of both normal (left) and inverse (right) electron-demand Diels–Alder cycloadditions.

nate with either the diene or dienophile to influence the HOMO–LUMO energy level gap. Reactions are consistently more favorable when the character of diene and dienophile are opposite (*i.e.* electron rich diene and electron poor dienophile, or *vice versa*.)

The interactions between the HOMO and LUMO govern the mode of reaction as well as the regiochemical outcomes, which can be critical when targeting specific structural isomers (*e.g.*, xylene, see Fig. 3). When asymmetrical addends (both diene and dienophile) are employed in Diels–Alder cycloadditions, two regioisomer cycloadducts can be produced depending on the orientation of addends during the reaction.[55] The preferred orientation of interaction occurs when the frontier orbitals of one addend that present the largest HOMO energy coefficient overlap with the frontier orbitals of the other addend that posses the largest LUMO energy coefficient.[56,57] The orbital coefficients are dependent on the electron-withdrawing or electron-donating nature of the substituents on each addend (see Table 1), and will drive the reaction to prefer certain regiochemical outcomes.

Stereochemically, the relative positions of substituents on the C_1 and C_4 positions of the diene and on the C_1 and C_2 positions of the dienophile are generally retained in the product due to the suprafacial nature of the addend interactions. In contrast, the newly formed stereocenters of the adduct are mediated by which of the two possible modes of suprafacial approach takes place: *endo* or *exo* (Fig. 4). Intuitively, one might assume that *exo* products are favored based on steric hindrance of *endo* interfacing. However, secondary orbital interactions that occur upon *endo* interfacing may result in stabilization of the transition state.[52,58] Accordingly, *endo* products are typically favored, a preference that is known as Alder's rule.[59] Through modification of reaction conditions or introduction of a bulky, chiral catalyst, stereochemical product distribution can be tuned to increase selectivity toward either stereoisomer.[60,61] However, for the production of aromatic compounds, stereocontrol of the cycloaddition is unnecessary due to the loss of all stereocenters within the cycloadduct during aromatization (Fig. 3).

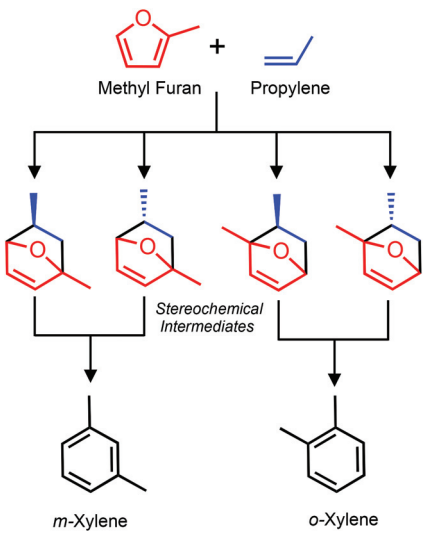

Fig. 3 Potential regiochemical and stereochemical outcomes of Diels–Alder cycloaddition between methyl furan and propylene. Subsequent dehydrative aromatization removes stereochemistry, but preserves regiochemistry.

Table 1 HOMO and LUMO energy coefficients for all dienes and dienophiles discussed within this review. Calculated using B3-LYP/6-311+G(d,p), ultrafine DFT grid, and tight SCF convergence. All characterized as positive definite minima structures by vibrational analyses

Diene	HOMO (eV)	LUMO (eV)
Furan	−6.531	−0.169
2-Methylfuran	−6.168	0.039
2,5-Dimethylfuran	−5.844	0.116
Butadiene	−6.702	−1.198
trans,*trans*-Dimethyl muconate	−7.623	−3.127
Isoprene	−6.515	−1.091
Dienophile	**HOMO (eV)**	**LUMO (eV)**
Ethylene	−7.660	−0.295
Propylene	−7.153	0.029
1-Butene	−7.154	−0.085
Maleic anhydride	−8.597	−3.591
Acrylic acid	−8.068	−1.927

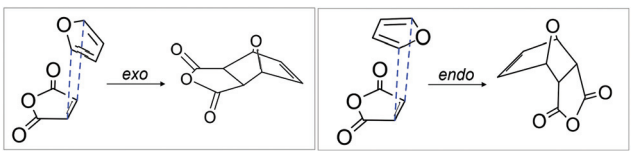

Fig. 4 Suprafacial interaction of Diels–Alder addends *via endo* (A) and *exo* (B) modes of molecular approach.

Role of acid catalysts for Diels–Alder reactions

As critical as catalysts are to enhance Diels–Alder reactions, it was not until the early 1940s that catalyzed Diels–Alder reactions were reported – over a decade after Diels and Alder first published their work.[62] Initially, homogeneous Brønsted acids (proton donors) were used to catalyze these cycloadditions.[63] However, it was shown in the early 1960s that homogeneous Lewis acid salts (electron pair acceptors) act as extremely effective catalysts that promote Diels–Alder reactions, even in mild reaction conditions.[64] Since the first records of acid-catalyzed Diels–Alder reactions, research into the use of Brønsted acids, Lewis acids, and tandem Brønsted–Lewis acids for these reactions has flourished. Increased efforts have focused on heterogeneous catalysts to improve recyclability and separations, and to enable continuous processing. However, the ability of homogeneous catalysts to exhibit high activity and extensive molecular modifiability has elicited in-depth studies into the catalytic principles that govern Diels–Alder reactions.

The enhancement of Diels–Alder reactions by acid catalysts is frequently described in terms of frontier molecular orbital (FMO) theory.[65–67] When an acid catalyst is present, it can

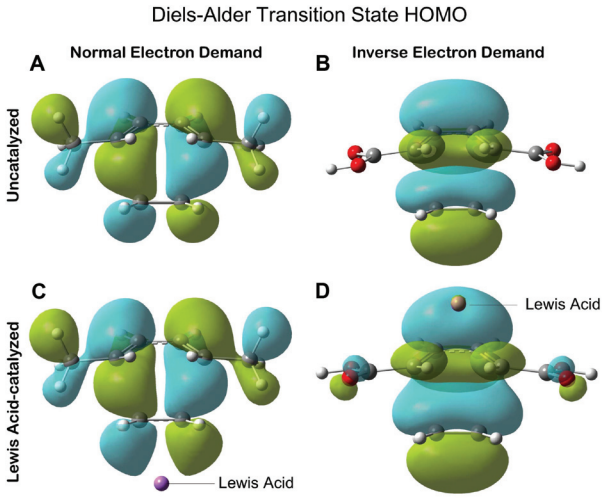

Fig. 5 Comparison of uncatalyzed (A, B) and Lewis-acid catalyzed (C, D) transition state HOMO orbitals for the NED Diels–Alder reaction of ethylene and 2,4-hexadiene (A, C) and the IED Diels–Alder reaction of *trans,trans*-muconic acid and ethylene (B, D). Catalyst depicted is cationic Li.

drastically decrease the HOMO–LUMO energy gap through coordination with sites of high electron density. In NED reactions, this corresponds to coordination of the acid with the dienophile (Fig. 5C), withdrawing electron density, and reducing the $LUMO_{dienophile}$. The resulting decreased energy separation between the $HOMO_{diene}$ and the $LUMO_{dienophile}$ enhances the susceptibility to nucleophilic attack by the π-electrons of the diene.[65,68] Likewise, in IED reactions, an acid catalyst will coordinate with an area of high electron density on the diene (Fig. 5D). This phenomenon can be observed in the NED cycloaddition of dimethylfuran with ethylene, for which it was shown that the $\Delta E_{HOMO-LUMO}$ is reduced from 182 kcal mol^{-1} to 26 kcal mol^{-1} upon introduction of cationic Li.[66] Several reports describe similar Diels–Alder reaction enhancement by addition of an acid catalyst.[69,70] In both NED and IED reactions, acid coordination enhances existing polarization of the molecule, increasing the associated orbital coefficient (Fig. 5), thus increasing the strength of orbital interaction between addends and promoting the reaction.[67]

Because acid catalysts typically enhance the existing reaction pathway (*e.g.*, decrease the energy gap between $HOMO_{diene}$ and $LUMO_{dienophile}$ in NED reactions), it would follow that the introduction of an acid catalyst also favors the enhancement of selectivity toward the major regio- and stereoisomer products.[65] In terms of Alder's rule, when small, non-sterically hindered catalysts are selected, this typically holds true and the *endo* product becomes even more strongly favored. However, use of bulky, chiral catalysts or those with size-restricted active sites can shift product selection toward the *exo* isomer due to insurmountable steric hindrance upon *endo* interfacing.[61] In literature, this has primarily been reported using homogeneous complexes. Moving forward, application of the principles governing stereochemical control by homogeneous catalysts to exemplary heterogeneous systems can potentially enhance the utility of catalysts designed for targeting stereospecific monomers *via* Diels–Alder chemistry, as discussed below.

Cooperative acid catalysis

To date, the synergy of Brønsted and Lewis acids for enhanced acid catalysis is accepted yet not fundamentally understood, and remains a topic of debate.[71,72] In the 1980s, around the time that this synergy was first observed, a suggested mechanism was proposed for the interaction in dealuminated zeolites. It was assumed that the interaction involved a partial electron transfer from the O–H bond of the Brønsted acid to the Lewis acid oxo-aluminum species. It was hypothesized that this interaction would increase the Brønsted acid site strength by reducing the strength of the O–H bond, much like what is observed within superacids. ^{1}H-NMR of a system in which this is occurring should illustrate a downfield chemical shift of the proton within the Brønsted acid site; however, it was later determined that no such shift is observed, indicating that is not the true method of interaction.[73] A more recent mechanism was proposed wherein no direct interaction occurs between the Brønsted and Lewis acid sites to invoke synergistic acidity.[74–76] Rather, it was reported that the spatial proximity of intramolecular Brønsted and Lewis acid sites affects the strength of the Brønsted acid by delocalizing the surrounding electron density, which increases the length and, thus, decreases the strength of the Brønsted acid O–H bond. Because of this interaction, the spatial proximity of the Lewis acid site to the Brønsted acid site has been shown to have a direct correlation with an increase in acid strength of the associated Brønsted acid site.[74,76]

In pursuit of exploiting the synergy between Brønsted and Lewis acid sites, "designer acids" can be synthesized for ideal catalytic behavior by affecting the catalyst–substrate interactions, reaction mechanisms, and/or shape-selectivity of the

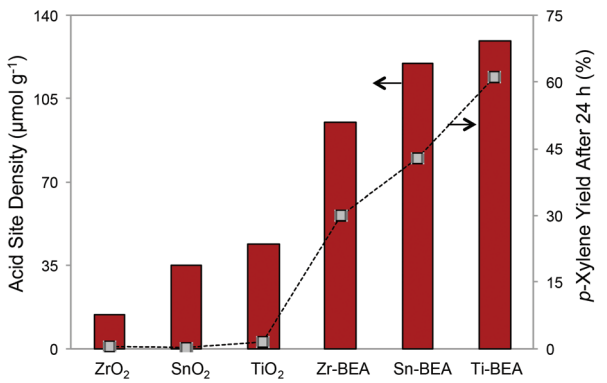

Fig. 6 Net yield of *p*-xylene in the tandem Diels–Alder and dehydration reaction of 2,5-dimethylfuran and ethylene catalyzed by a series of metal oxides and their zeotypic analogs. Net *p*-xylene yield after 24 h of reaction correlates strongly with increasing acid site density. *p*-Xylene yield reported on a total carbon yield basis.[45]

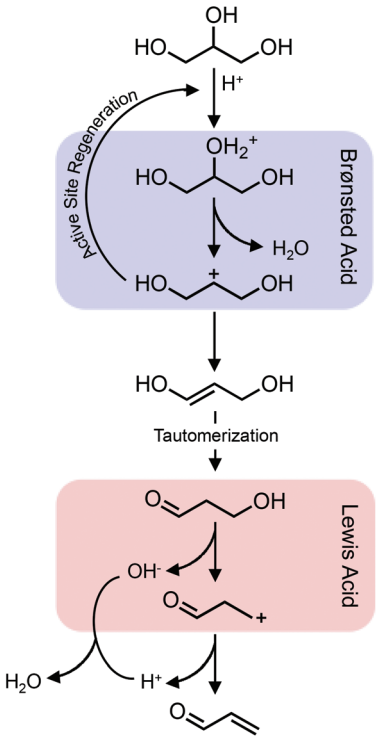

Fig. 7 Illustrative reaction of Brønsted and Lewis acid synergy for production of acrolein from glycerol. Reported yield >54% over Al/H-ZSM-5.[75]

catalyst system (Fig. 7).[77] These effects have been investigated for catalysis of Diels–Alder reactions, for which several types of combined acids have been indicated, including: Brønsted acid assisted Lewis acids (BLA), Lewis acid assisted Lewis acids (LLA), Lewis acid assisted Brønsted acids (LBA), and Brønsted acid assisted Brønsted acids (BBA).[61] The variety in possible Brønsted–Lewis acid site interactions allows for further tailored catalysts based on the desired primary acidity. BLA catalysts are specifically of interest for applications in targeted aromatics from biomass due to precedence of Lewis-acids as notably successful catalysts for Diels–Alder reactions. This effect was illustrated in the Diels–Alder reaction of naphthoquinone derivatives and varying dienes using a BLA catalyst, which resulted in both rate enhancement and increased stereoselectivity due to modified reactant–catalyst interfacing by the acid sites.[61]

Tandem Diels–Alder and aromatization reactions

In order to target aromatic monomers, Diels–Alder cycloadditions require subsequent aromatization. This is typically accomplished *via* dehydration or dehydrogenation reactions, although reactions such as decarboxylation[78–80] can be used to impart aromaticity for certain cycloadducts. In order to facilitate tandem Diels–Alder and aromatization reactions, multifunctional materials capable of catalyzing both reactions can be particularly useful (Fig. 6). Tandem reactions over a single catalyst have the potential to increase yield and atom efficiency while circumventing the need for separations of functionally complex, reactive, or harmful intermediate compounds. Additionally, one-pot reactions may facilitate enhanced yields relative to the multi-system alternatives due to lack of isolation and separations between reaction steps. For example, the combined Diels–Alder dehydration of 2,5-DMF with ethylene for *p*-xylene production has been reported at net yields of 90%.[45] When performed in separate reaction systems, the production of *p*-xylene through a Diels–Alder reaction scheme suffers from low net yields of only 30–34% and significant byproduct formation due to the reactive oxanorbornene intermediate.[81]

Regarding dehydration, catalytic mechanisms for Brønsted acids, Lewis acids, and metal oxides that display Brønsted and/or Lewis acid activity have been described in literature. Brønsted acids are the most well documented catalyst for dehydration reactions, and they may initiate one of several mechanistic pathways based on substrate functionality. In the case of bridging ethers, such as those in oxanorbornene-type Diels–Alder cycloadducts produced upon addition with furanic compounds, the reaction has been reported to proceed through simultaneous protonation of the oxygen and cleavage of one ether C–O bond (Fig. 8A). Subsequently, proton transfer to neutralize the resulting carbocation facilitates the formation

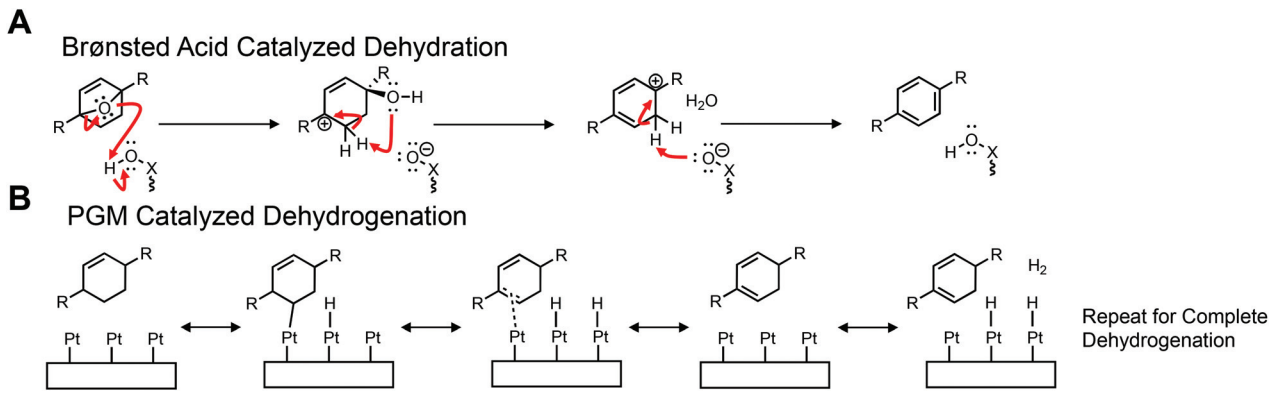

Fig. 8 Demonstrative mechanisms for generation of aromaticity in cycloadducts *via* Brønsted acid catalyzed dehydration (A) or PGM catalyzed dehydrogenation (B).

of one olefin bond within the cycloadduct. A second proton abstraction to the cleaved ether oxygen drives water dissociation from the cycloadduct, cleaving the remaining ether C–O bond. When the second bond is cleaved, an additional olefin bond is formed by proton transfer within the ring, resulting in complete aromatization of the cycloadduct.[82] Through a similar mechanism, Lewis acids may catalyze oxanorbornene dehydration.[83] A recent computational study investigated the Lewis acid catalyzed dehydration mechanism for the production of *p*-xylene by Diels–Alder cycloaddition of 2,5-dimethylfuran (2,5-DMF) with ethylene.[66] The major difference between the Brønsted acid catalyzed mechanism and the Lewis acid catalyzed mechanism was observed to be the mode of initial C–O bond cleavage. Rather than directly protonating the C_1–C_4 bridging oxygen as a Brønsted acid does, it was hypothesized that Lewis acid sites withdraw electron density from the bridging oxygen and facilitate a shift of one C–O bond, relocating the C–O–C bridge to C_1 and C_2 of the six-membered ring. Subsequently, there are two proton transfers, as described for the Brønsted acid-catalyzed mechanism.[84] The second proton transfer allows final C–O bond cleavage, releasing H_2O. Although less frequently reported, acidic metal oxide catalysis of dehydration reactions is also feasible.[85] The mechanism begins with coordination of oxygen to a metal site within the oxide, in the same manner as Lewis acid catalyzed dehydration. Following coordination, the oxygen atoms adjacent to the metal site aid in the necessary two proton transfers. Upon the second proton transfer within the ring, water is released from the now-aromatic ring.

In contrast to dehydration, the most commonly described dehydrogenation mechanisms involve platinum group metals (PGMs, Fig. 8B), although transition metal oxides and acidic zeolites have also been reported for catalysis of dehydrogenation reactions. Within metal oxide frameworks, it has been suggested that alkane dehydrogenation begins through coordination of an alkane carbon with a coordinatively unsaturated metal site.[86] Simultaneously, a hydrogen atom is transferred from the alkane carbon to an oxygen adjacent to the metal center. A second hydrogen transfer from the alkane to the metal center facilitates formation of the alkene, which then desorbs from the catalyst surface. At this state, hydrogen atoms from the alkane are coordinated to both the metal center and an adjacent oxygen, which then associatively desorb as an H_2 molecule, regenerating the active catalyst surface. The catalytic mechanism of dehydrogenation over PGM surfaces is similar to that over metal oxides. On PGM surfaces, the coordination of an alkane carbon to a metal site is followed by hydrogen transfer to a neighboring metal site, rather than to an oxygen as observed over metal oxides. Formation of the alkene drives transfer of a second hydrogen to another adjacent metal site and desorption of the olefin product. Desorption of hydrogen from both metal sites regenerates the active surface while releasing molecular H_2. Comparatively, the mechanism of dehydrogenation over Brønsted acidic hydroxyl groups of zeolites is significantly different than that of metal oxides or PGMs and has been proposed to proceed through a carbocation-based mechanism.[87–90] The protonation of an alkane carbon by the Brønsted acidic hydroxyl group initiates the reaction, forming a penta-coordinated carbocation. The carbocation proceeds to coordinate with the zeolitic oxygen, allowing the formation of an alkene bond within the substrate that drives the simultaneous release of molecular H_2 from the penta-coordinated carbon. After alkene formation and H_2 release, the olefin dissociates from the catalyst surface, completing the reaction.

Due to the ability of several catalytic materials to facilitate dehydration and dehydrogenation, multifunctional catalyst materials show promise to facilitate tandem Diels–Alder and aromatization reactions. Herein, the potential for zeolitic materials and polyoxometalates (POMs) to address this need is discussed, as they are two exemplary, tunable, solid acid catalysts.

Zeolites

Developing heterogeneous catalyst systems is of significant interest to promote continuous flow reactor operations for Diels–Alder chemistry and facilitate cost-effective industrial processes for commodity aromatic production.[91] Zeolites are crystalline, porous aluminosilicates that can take on over 229 different structural configurations and countless modifications through heteroatom framework substitutions (Fig. 9).[92] This allows for tuning of zeolite active sites,[93–95] with several studies demonstrating the enhancement of Diels–Alder reactions using synergistic Brønsted–Lewis zeolitic catalysts. Examples include the Brønsted–Lewis acid zeolite-catalyzed cycloaddition of 2,5-DMF with ethylene and subsequent dehydrative aromatization to produce *p*-xylene.[96] Similarly, tandem Diels–Alder cycloadditions and dehydrations for toluene and benzoic acid production have been performed with dual-acid zeolite catalysts.[97,98] In addition to their ability to catalyze Diels–Alder reactions, zeolites may promote relevant aromatization reactions. The ability of H-Beta zeolite as a dehydration catalyst was described for the tandem isomerization-dehydration of biomass-derived gamma-valerolactone (GVL) to furfural.[99] Additionally, the dehydration ability of zeolites for

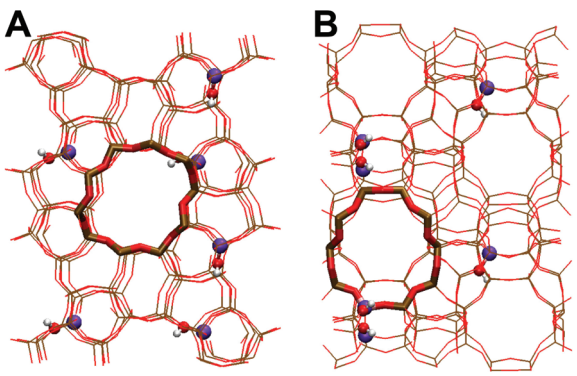

Fig. 9 Structural depiction of heteroatom-substituted H-ZSM-5, a representative zeolite catalyst, shown along the straight channel (A) and zig-zag channel (B).

the *in situ* conversion of ethanol to ethylene during Diels–Alder reactions with furans has been described.[100] While less investigated, zeolites can also catalyze dehydrogenation reactions. A recent publication illustrated the use of Cr/ZSM-5 for oxidative dehydrogenation of ethane,[101] and a well-know 1993 study exemplified the ability of ZSM-5 to dehydrogenate methane for benzene production.[90] Many literature reports of zeolite-catalyzed dehydrogenation of partially saturated cyclic structure involve oxidative dehydrogenation,[102–104] though there are reports of non-oxidative dehydrogenation of such species by modified zeolites.[105–107]

Because of the tunability of zeolites, most in-depth investigations of Brønsted–Lewis acid synergy to date have been conducted on this class of materials. Brønsted acid sites in zeolitic materials are a result of bridging hydroxyl groups (Si–OH–Al) and four-coordinate framework Al. In contrast, Lewis acid sites are due to extra-framework Al sites or framework Al that is three-coordinate. Partial dealumination of various zeolites (*e.g.*, Y, ZSM-5, Beta, MOR) results in partial release of Al and an increased number of extra-framework Al sites, increasing the Lewis acidity of the zeolite. However, the increased acidity of partially dealuminated zeolites is much larger than would be expected if only due to increased Lewis acidity. Literature reports identify a synergy between the Brønsted acid sites and extra-framework Al Lewis acid sites that is responsible for the observed increased catalytic ability.[73,76,77,96] It has been repeatedly proposed that the spatial proximities of the Brønsted acid sites to the Lewis acid sites within zeolitic frameworks strongly correlates with increased acidity. In the case of modified dealuminated H-MOR and dealuminated H-ZSM-5, ^{13}C-NMR of absorbed acetone, a well-established probe molecule for measuring Brønsted acid strength, was used to illustrate that Brønsted acid strength significantly increased by the presence of a proximal Lewis acid site.[74,76] Based on the observed acid site interactions, two modes of tandem reactivity have been proposed: Lewis-acid catalyzed Diels–Alder and subsequent Brønsted acid-catalyzed aromatization, or dual Brønsted–Lewis acid site-catalyzed Diels–Alder and aromatization reactions. To date, it has been hypothesized that the mode of catalysis that occurs is highly dependent on the specific catalytic system and reaction scheme.

Heteropolyacids/polyoxometalates

Similar to zeolites, POMs are highly tunable, discrete molecular catalyst species that can be modified to target catalytic activity for Diels–Alder and aromatization reactions. POMs are composed of large metal–oxygen cluster species with a diverse compositional rage and great structural variety. Typically, POMs are formed around early transition metals (*e.g.*, W, Mo) in their highest oxidation states (Fig. 10). Under the classification of POMs, heteropolyacids (HPAs) are specifically those in which the counterion is a proton. While POMs are based on metal–oxygen frameworks, they present a well-defined molecular structure rather than a solid crystalline expanse like zeolitic materials. Typically, POM molecules contain a central heteroatom surrounded by a transition metal–oxygen framework composed of polyhedral units. Unlike zeolites, POMs do not have distinct pores. However, the lacunary POMs may be prepared *via* removal or modification of polyhedral units and catalysis may occur within the vacant sites similar to the manner in which catalysis occurs in zeolitic pores.[108,109]

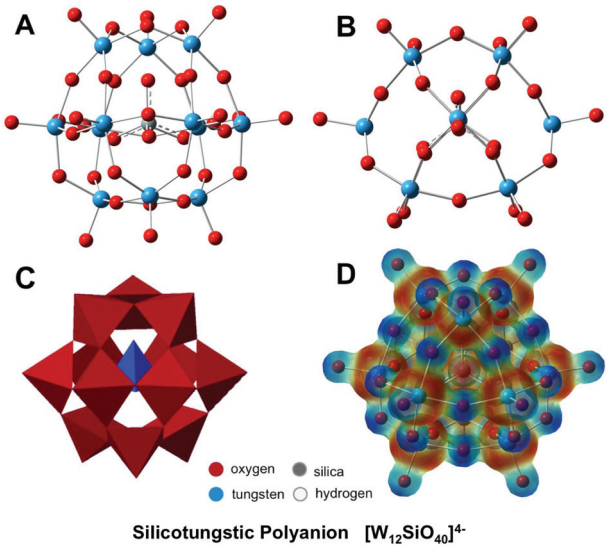

Fig. 10 Structural depiction of silcotungstic acid, in its polyanion isomer (A), viewed along a symmetry plane (B), crystallographic space-filling model (C), and the u-B3LYP/Def2-SVP calculated molecular electrostatic potential mapped to the total electron density surface of isosurface value 0.1 (D).

POMs are not only bifunctional, but may also be considered tri- or tetra-functional due to the presence of oxygen atoms, protons, and metals, providing soft basicity, Brønsted acidity, Lewis acidity, and redox capabilities.[109] POMs can be considered "designable" as well, due to the tunability of several aspects of the POM molecule.[110] Due to their solubility in polar solvents, most POMs are not inherently heterogeneous catalysts. This excludes some salts of POMs, such as cesium salts, which are insoluble and can be employed as heterogeneous catalysts without a support.[111] Or, POMs can be effectively supported over several high surface area materials.[112]

To date, POMs are primarily utilized catalytically in an unmodified, Brønsted acid-dominant state[113] (*i.e.*, the native acid sites have not been altered to achieve targeted Brønsted acid/Lewis acid ratios for enhanced activity). Although minor Lewis acid character does exist within POMs in their native state, transition metal-substituted heteroatoms can impart greater Lewis acidity.[71] Based upon the known utility of Lewis acids for Diels–Alder cycloadditions, it is expected that increased Lewis acidity will promote these reactions further, while the retained Brønsted acidity will promote aromatization reactions. However, the use of POMs that have been modified in this manner has not yet been studied extensively for Diels–Alder purposes. Additionally, although headway has been made in the elucidation of the mechanism of cooperative catalysis amongst zeolitic species, no analogous explanation has been proposed for POMs to date.

Like zeolitic materials, research efforts have illustrated the capacity of POMs as catalysts for Diels–Alder reactions, which is significant for the reactions discussed throughout this review.[112,114,115] For example, it was recently illustrated that silicotungstic acid, a Keggin-type HPA, effectively catalyzes the Diels–Alder cycloaddition of *trans*,*trans*-diethyl muconate with ethylene.[114] POMs have been also been utilized for aromatization reactions that would be necessary following cycloaddition. The dehydration of bio-ethanol to ethylene was completed in high conversion and selectivity by montmorillonite-supported dodecatungstophosphoric acid.[116] Additionally, metal organic framework (MOF) encapsulated phosphotungstic acid was shown to effectively catalyze the dehydration of fructose and glucose to 5-hydroxymethyl furfural (5-HMF).[117] Furthermore, POMs can be effective for dehydrogenation reactions, although they are less frequently utilized.[112] Their capacity for oxidative-dehydrogenation is well studied, while non-oxidative dehydrogenations are reported less often. However, POM frameworks are capable of possessing Lewis acidity, Brønsted acidity, bridged metal–oxygen sites, and can support platinum group metals. Making use of this tunability has been successful for promoting the dehydrogenation of cyclohexanol by vanadium-substituted Wells–Dawson type POMs.[118] As evidenced, the modifiability of POMs allows for multifunctionality that may be utilized for tandem Diels–Alder and aromatization reactions.

Insight from computational chemistry

The strengths of theoretical methods include the ability to evaluate elusive characteristics such as transition state structures, direct comparisons of concerted *versus* stepwise mechanisms, and the origins of stereoselectivity (Fig. 11). Early computational approaches supported that bond formation in the cycloaddition of butadiene and ethylene adopts a concerted mechanism,[51] whereas a stepwise mechanism has been also implicated for diverse addend pairs.[53] With numerous exceptions arising, the discussion regarding mechanism has been frequently revisited. In all of these investigations, probable mechanisms are supported by electronic structure calculations yielding the relative stabilities of the transition state geometries, and by evaluating energetic differences of various electronic configurations. For example, a concerted mechanism of singlet state reactants remains a singlet ground state throughout the reaction pathway, in contrast to a stepwise mechanism, which may involve a paired-electron transition state towards each bond formation, or may potentially feature a more stable biradical intermediate. Pairing the transition state predictions to the free energies of the addends and cycloadducts as well as interaction energies to bring together the reaction complex, a full reaction profile may be constructed to identify rate-limiting steps and rationalize more effective addend pairs or catalysts. From this insight, reaction parameter adjustments that will better stabilize the transition state of the rate-limiting step may be clearly targeted.

Efforts continue to develop more robust predictive computational models for the ever-expanding diversity of cycloaddition addends and catalysts. While offering excellent correlations for NED cycloadditions that lack heteroatoms, FMO theory was, in contrast, found to yield poor predictions and correlations for cases of IED cycloadditions, or in reactions where asymmetry of the addends and orbital overlap play a greater role than the HOMO–LUMO energy gap.[119] The frequency of such deviant cases stimulates the ongoing development of theoretical strategies to best correlate observed reactivity to a particular, more concise electronic property. To amend these theoretical discrepancies, new correlative approaches including the calculation of reactive molecular orbitals,[120] and TS distortion energy models have been recently developed.[121–123] For cases involving IED mechanisms or cycloalkenes, these models achieved more reliable correlations to activation energies and experimental observations than FMO theory alone.

In silico catalyst design

In addition to calculating the reactivity of uncatalyzed Diels–Alder adducts, *in silico* screening can efficiently compare a

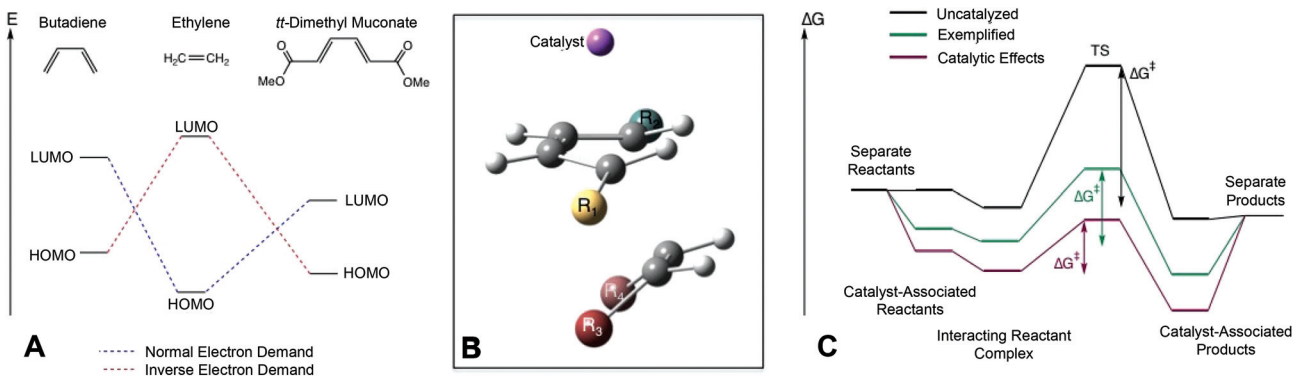

Fig. 11 Common strategies for computational investigation of Diels–Alder reactivity through impacts on frontier orbitals due to addends or catalyst interactions (A), substituents or catalyst stabilization of the transition state structures (B), and free energy profiles for catalyst and addend association, transition and product formation (C).

suite of catalysts, towards the reduction of time and costs of reaction optimization. Computational prediction and design of small catalysts, including organocatalysts and organometallic catalysts, has gained considerable momentum in many research communities, particularly as modern advances in DFT and supercomputing resources have made it tractable to model larger inorganic catalyst-reactant complexes.[124–126] Instead of exclusively relying on synthetic experiments, calculations of the free energies and orbitals through various catalyzed reaction steps has the potential to quickly and inexpensively determine what substituents or interactions are necessary for effective catalysis and provide rational design guidelines. Hypothesized modifications of addend or catalyst moieties may also be screened computationally by comparing these variations in a resolved transition structure serving as a template; this effectively enables the screening of ligands and substituents to evolve more effective catalysts.

Among the accumulating successes in rational catalyst design, several studies have demonstrated the power of computational prediction for cycloadditions. The computational design of a rhodium catalyst, for example, was experimentally confirmed to facilitate a multicomponent [5 + 2 + 1] cycloaddition to a cyclooctenone product.[127] Also successful were exemplary models of oxazaborolidine catalysts, which clarified the strong experimentally-observed stereospecificity with a robust DFT mechanistic evaluation on five dienophiles.[128,129] In a third example, a rhodium catalyst was computationally explored to reveal the basis of high *para*-selectivity of cycloaddition with alkynes, and how an additional coordination of the alkyne with rhodium—relative to the catalyst interaction with alkenes—results in a higher reaction rate.[130]

Recent works have initiated models of Lewis-acid catalyzed Diels–Alder reactions, in which cations of Li, Na, K, Rb, and Cs served as the catalytic acids coordinating to either 2,5-DMF or ethylene.[66] These computational works have greatly contributed towards the understanding of Lewis acid-catalyzed upgrading of biomass-derived 2,5-DMF. Furthermore, these studies have initiated a wave of new efforts to computationally evaluate and clarify reactivity and properties of zeolite catalysts specifically for cycloaddition chemistry.

Esteemed for high variability and tunability, zeolites have gained broad interest as multipurpose catalytic scaffolds for a diverse spectrum of chemical transformations, particularly where interest lies in heterogeneous catalytic approaches amenable to efficient industrial processes. More recently, the utilization of zeolites for Diels–Alder catalysis has been the target of computational works with both free Lewis acid cations[66] as well as Lewis acids that are explicitly confined within a zeolite framework.[96,131] The latter works often apply quantum mechanics/molecular mechanics (QM/MM) calculations to take into account the surrounding zeolite structure, and to examine the effects of steric constraints on the reaction when it occurs within the zeolite pores. In these models, the confinement effects as well as charge transfer were found to play key roles in achieving enhanced efficacy of the cycloaddition as well as the subsequent dehydration reaction. Other studies employing QM/MM strategies support these findings of reduced activation energies for cycloadditions confined within alkali-exchanged zeolites.[132,133] Interestingly, when considering tandem Diels–Alder and dehydration reactions, the rate-limiting step was found to be dependent upon the acid site concentration within the zeolite, with the cycloaddition as the limiting step for low acid site concentration within the zeolite.[25] Further mechanistic insight suggests that the zeolite framework alters the Lewis acid cation's capacity to withdraw electron density from 2,5-DMF, resulting in a nearly electronically-neutral bidirectional electron flow, as opposed to either a NED or IED mechanism.[25] Long-range electrostatic interactions were, however, not considered in these models, which would be important to address in future works to achieve quantitative binding enthalpies.

Computational models have also recently advanced for another attractively malleable catalytic scaffold, polyoxometalates, which possess highly versatile acid sites and redox chemistry capabilites.[109] POMs and their conjugate heteropolyacids may undergo single-site modifications and isomerizations that alter their catalytic activity substantially, demonstrating their adaptability, which has rendered them useful to catalyzing an impressive range of chemical transformations. Again benefitting from advances in DFT calculations, the use of theoretical models to study POMs has bloomed just since the turn of the century.[134] Although the computational evaluation of POMs is steadily gaining momentum, no computational works have been published to date on the application of POM catalysts in cycloaddition chemistry to the best of our knowledge. However, the path forward with POM adaptation looks promising, as with the zeolite frameworks, to tailor these highly tunable catalysts for heterogeneous Diels–Alder reactivity.

Direct replacement aromatics

The conversion of petroleum to aromatic monomers has been developed over decades to become highly efficient and cost-effective. Petroleum-derived hydrocarbon aromatic monomers (*e.g.*, BTX) are recovered from crude oil refining, while oxygenated aromatics (*e.g.*, benzoic acid, phthalic acid, terephthalic acid) are produced from the successive addition of oxygen to BTX fractions.[135] In contrast, the production of hydrocarbon aromatic monomers from lignocellulosic biomass requires extensive deoxygenation, as biomass has an inherently high oxygen content ranging from 30–40% by mass.[136,137] This allows for potentially higher atom efficiencies when targeting oxygenated aromatics if oxygen can be retained during conversion.[137] Recent life cycle assessments of biobased compounds have indicated that, with proper feedstock selection and improved processing, the production of many compounds can require less energy and exhibit cost competitiveness when compared to the analogous petroleum-based processes. For example, butanediol production has an estimated 83% greenhouse gas emission and 46% reduction in nonrenewable energy use.[138] Several of these routes, however, require

improvement to be viable. Largely, feedstock cost is the driving factor that impacts final product cost, making yield from each unit process critical. For example, a techno-economic analysis of *trans*-3-hexenedioic acid production from biomass illustrated that a 1% change in the fermentation yield of the intermediate compound, muconic acid, results in 1% a change in the overall market price.[139] In general, the competitiveness of biomass-derived commodity aromatics *via* Diels–Alder chemistry will ultimately be dictated by the efficient production of addends and their subsequent conversion to cycloadducts.

Numerous routes have been investigated for the production of Diels–Alder addends from biomass (see Fig. 12 and 13), including (1) chemocatalytic processing, (2) biological processing, and (3) hybrid processing. Chemocatalytic processing typically relies on homogeneous or heterogeneous inorganic catalysts and has primarily focused on the high-yield production of furans and their derivatives. Conversely, biological transformations can support a wide diversity of products with incredibly varied functionalities. Lastly, linking chemical and biological transformations *via* hybrid processing has been shown to greatly augment the number of Diels–Alder addends accessible from biomass. Illustrative examples of the methods for producing biomass-derived intermediates and commodity aromatic compounds by these routes are provided below.

Toluene

In 2015, global toluene consumption was estimated at over 23 million metric tons, with expected growth to 28 million metric tons by 2020.[140] The applications of toluene are diverse, including use in paints, glues, printing ink, adhesives, cosmetics, and as an industrial solvent. Traditionally, toluene is isolated from petroleum reformate using a liquid–liquid extraction process. This process first involves the simultaneous extraction of all aromatics present in the mixture while displacing non-aromatics. An extraction column is utilized for this process, in which a selected solvent is introduced at the top of the column and the mixture is injected into the middle of the column. The non-aromatics leave at the upper end of the column and the solvent, now containing the aromatics, is removed at the bottom of the column. Subsequent isolation by

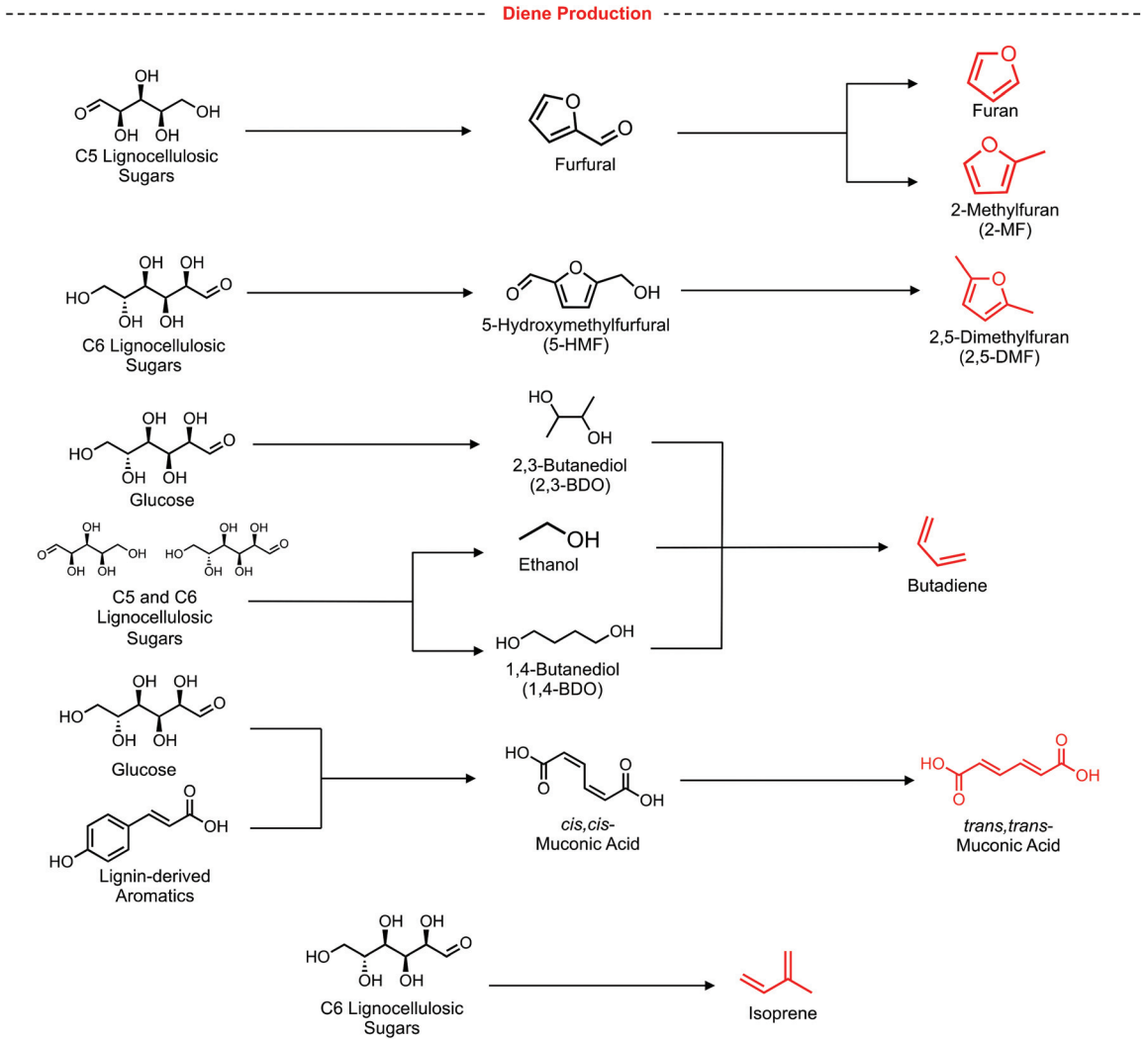

Fig. 12 Illustrative examples of production routes for common dienes from biomass or biomass-derived starting materials.

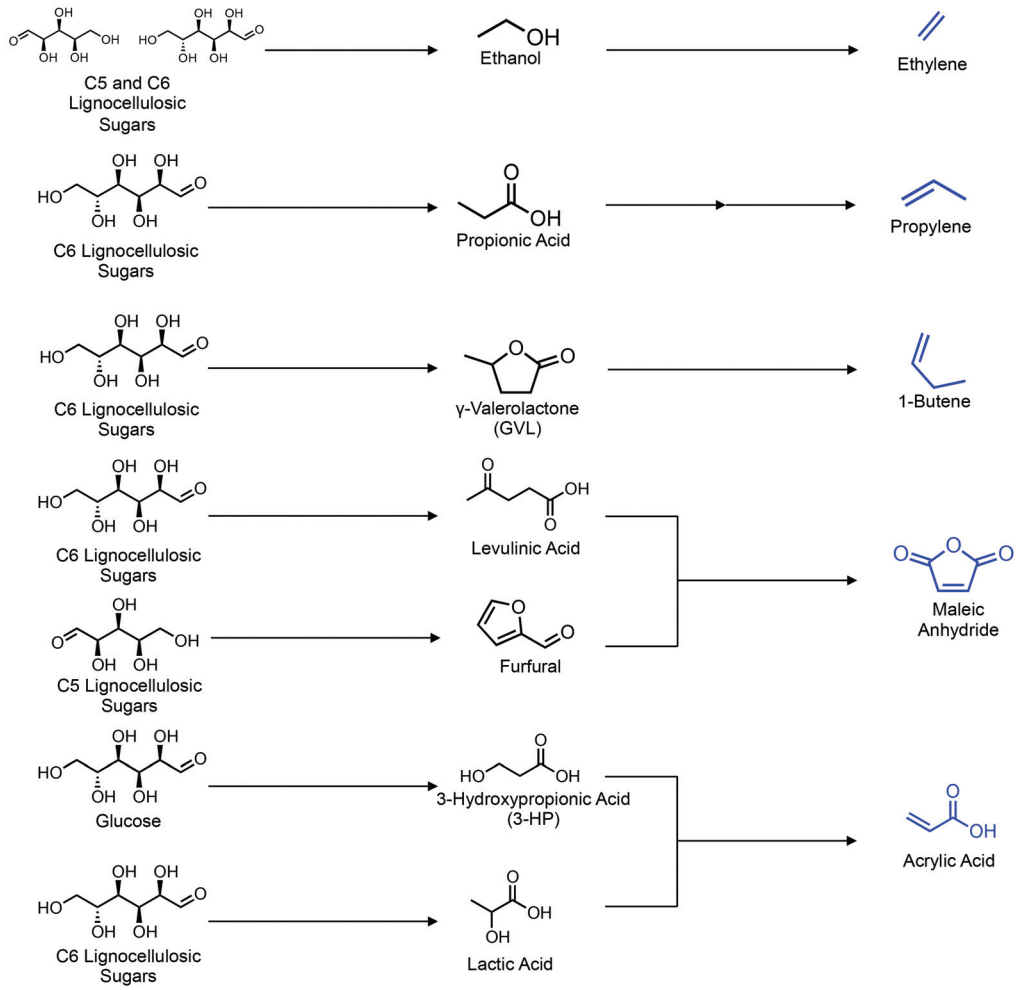

Fig. 13 Illustrative examples of production routes for common dienophiles from biomass-derived starting materials.

steam stripping of distillation results in toluene yields of up to 98.5%.[135]

Diels–Alder production of biobased toluene. Through Diels–Alder cycloaddition and dehydration, toluene can be produced renewably from 2-methylfuran (2-MF) and ethylene, or furan and propylene (Fig. 14). In 2015, the global production of biomass-derived furfural was over 440 000 metric tonnes, will projected growth to nearly 550 000 metric tonnes by 2020.[141] For batch reactions of 2-MF with 30 bar ethylene over alkali-exchanged Y zeolites in the presence of a Lewis acid salt, yields up to 70% have been reported using a reaction temperature of 250 °C for 8–24 h.[98] The same reaction performed between 200–275 °C with 14 bar ethylene using BEA zeolites without the presence of Lewis acids has been reported at a net yield of only 46% due to side production formation,[142] underscoring the importance of multifunctional catalyst systems. The tandem cycloaddition-dehydration of furan and propylene for toluene production has also been reported using zeolite catalysts, namely unmodified ZSM-5, with reported net yields

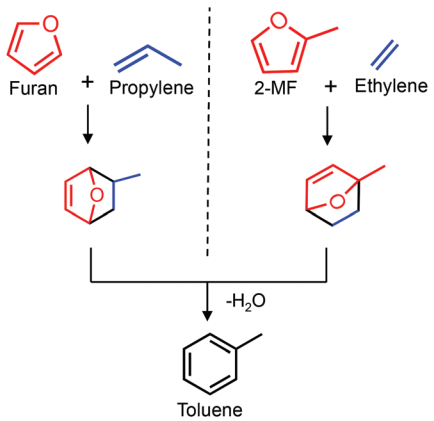

Fig. 14 Diels–Alder cycloaddition and subsequent dehydrative aromatization of biomass-derived addends for production of toluene.

of over 20% under atmospheric pressure with harsh temperatures of 400–650 °C in continuous flow reactions.[143] While incorporation of Lewis acids in this reaction may increase yield due to mitigation of side product formation, no reports of dual Brønsted–Lewis acid systems have been reported.

Chemocatalytic production of intermediates. A net yield of 98% 2-MF has been reported from dehydration of pure xylose streams to furfural over H-zeolite catalysts (*e.g.*, H^+ mordentite), followed by hydrogenation to 2-MF over a Cu/Fe catalyst.[144] In separate systems, the production of furfural and the hydrogenation of furfural to 2-MF have both been reported in very high yields; up to 92% yield of furfural from mixed lignocellulosic pentoses has been reported using strong Brønsted acid catalysts.[145] Hydrogenation of furfural to 2-MF, a process that has been known since the 1940s, has been achieved at yields upwards of 90% using a variety of catalytic materials including copper chromite, bifunctional Ru/RuOx/C, and modified zeolites.[146,147] Through an alternative decarbonylation route, furfural can be converted to furan in high yield, such as in the use of K-doped Pd/Al_2O_3 catalyst to achieve yields of over 99%.[148]

Hybrid production of intermediates

Both ethylene and propylene may be produced through a hybrid chemical-microbiological production route that begins with a fermentative process. The fermentation of lignocellulose hydrolyzate by *Propionibacterium acidipropionici* for propionic acid has been reported in literature with titers as high as ~135 g L^{-1},[149,150] followed by reduction to 1-propanol using palladium catalysts with yields of 30%.[151] Subsequent dehydration of 1-propanol to propylene over catalysts ranging from zinc aluminates to various acid catalysts have been reported with yields of up to >99%.[152] The production of ethylene involves a well-developed method of bioethanol preparation *via* fermentation of biomass, followed by dehydration to ethylene. Current technologies can achieve bioethanol yields upwards of 90% theoretical.[23,153,154] Subsequent catalytic dehydration of bioethanol to yield ethylene in yields of up to 99% have been reported.[155] In addition, direct biological production of ethylene has been described using an ethylene-forming enzyme.[156,157]

para-Xylene

In 2015, the global consumption of mixed xylenes (*o*-xylene, *m*-xylene, and *p*-xylene) was reported to be over 52 million metric tons with forecasted growth to over 65 million metric tons in 2020.[158] Of the reported global consumption of xylenes in 2015, nearly 37 million metric tons was attributed to *p*-xylene, exclusively.[158] *p*-Xylene is primarily used as a raw material for terephthalic acid production *via* oxidation, and is subsequently polymerized with ethylene glycol to produce PET. The demand for *p*-xylene has increased as the commercial use of PET has surged, primarily in the bottling industry. Petroleum-derived *p*-xylene is purified from petroleum reformate, which is made up of approximately 20% mixed xylenes. In order to isolate *p*-xylene, a first-stage separation from non-aromatic species followed by isolation *via* crystallization is utilized. The mixed fraction that results from the initial stage of separations contains all three xylene isomers as well as ethylbenzene.[159] Due to similar boiling points, *m*-xylene and *p*-xylene (boiling points of 139.1 °C and 138.3 °C, respectively) are the most difficult components of this mixture to isolate. A fractional distillation for these two compounds would require over 800 theoretical plates, and is not economically reasonable. Therefore, separation by freezing is utilized as an alternative means of separation.[160] The separation of all four components (xylene isomers and ethylbenzene) in this mixture first involves removal of *o*-xylene and ethylbenzene by conventional fractional distillation based upon these species' distinctly higher and lower boiling points (144.4 °C and 136.2 °C, respectively). The *m*-/*p*-xylene mixture is then cooled slowly to between −20 °C and −75 °C. *p*-Xylene crystallizes first and is removed from the system. Through a series of re-melting and freezing, *p*-xylene with up to 99.5% purity may be obtained. The *m*-xylene fraction typically has lower purity, is isomerized to *p*-xylene, and undergoes a second round of crystallization to isolate as much *p*-xylene as possible from the initial reformate fraction.[135]

Diels–Alder production of biobased *p*-xylene. The cycloaddition of 2,5-DMF with ethylene and subsequent dehydration is a well-developed Diels–Alder route of *p*-xylene production (Fig. 15). While separate Diels–Alder cycloaddition and dehydration reactions have been reported, the Diels–Alder reaction typically suffers low selectivity due to reactivity of the intermediate leading to non-target by-product formation. However, using Lewis acid-modified zeolites for the tandem Diels–Alder dehydration reaction circumvents isolation of the reactive intermediate, facilitating higher yields. Several research groups have illustrated this, using modified BEA zeolites to achieve *p*-xylene yields between 90–97%.[42,45,97] The highest net yield of 97% was achieved using phosphorous-modified zeolite BEA in batch reactions at 250 °C under 62 bar ethylene.

Chemocatalytic production of addends. The production of 2,5-DMF from biomass first requires the dehydration of biomass-derived C_6 carbohydrates to 5-HMF, followed by

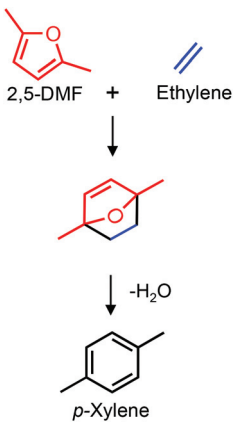

Fig. 15 Diels–Alder cycloaddition and subsequent dehydrative aromatization of biomass-derived addends for production of *p*-xylene.

hydrogenolysis to 2,5-DMF. A net 2,5-DMF yield of 72% in a continuous reaction system using aqueous fructose as the starting material was recently reported.[161] In this reaction scheme, mineral acids (*e.g.*, HCl) catalyzed dehydration to 5-HMF and CuRu/C catalysts facilitated hydrogenolysis. Furthermore, a recent report identified a method for producing 5-HMF at a yield of 79% from raw lignocellulosic biomass using a dilute NaOH pretreatment of the biomass, followed by conversion to 5-HMF using a chromium chloride catalyst.[162] Likewise, other reports have identified catalytic methods of converting raw biomass to 5-HMF with similar yields.[163,164] Isolated 5-HMF can then be chemocatalytically converted to 2,5-DMF in desirable yield, as shown with a PdAu/C, HCl catalyst system to achieve 2,5-DMF yields of 99%.[165]

Hybrid production of addends. As described previously, ethylene can be produced through a hybrid pathway that first involves fermentation of biomass to produce ethanol, followed by catalytic dehydrogenation of ethanol to ethylene.

Ethylbenzene

Nearly all ethylbenzene is utilized for production of the large-market commodity monomer, styrene. Because of this in-demand application, the global consumption of ethylbenzene was over 29 million metric tons in 2014, with anticipated growth to 32 million metric tonnes by 2019.[166] Styrene is used in a wide variety of polymeric materials, such as polystyrene, acrylonitrile-butadiene-styrene (ABS), and fiberglass reinforced plastics.[167] While ethylbenzene can be directly isolated from petroleum reformate in the same manner as toluene, most ethylbenzene used commercial is manufactured by the alkylation of benzene.[159] Benzene can be isolated from petroleum reformate or pyrolyzate using liquid–liquid extraction in yields of up 99.9%. Subsequently, it is alkylated to ethylbenzene using either liquid phase ethylation with Friedel–Crafts catalysts, or gas-phase ethylation catalyzed by supported H_3PO_4 or aluminum silicates.[135]

Diels–Alder production of biobased ethylbenzene. Ethylbenzene can be produced through Diels–Alder addition using a series of different dienes and dienophiles, which may be (1) 1,3-butadiene only, through Diels–Alder dimerization and subsequent dehydrogenation, (2) 1,3-butadiene and 1-butene with subsequent dehydrogenation, or (3) furan and 1-butene with subsequent dehydration (Fig. 16). Route (1) has been illustrated using an open-framework nickel-phosphate for the production of ethylbenzene at low conversion with over 80% selectivity in a continuous flow reactor at atmospheric pressure and an operating temperature of 400 °C.[168] To our knowledge, routes (2) and (3) have not been successfully reported in the peer-reviewed literature.

Chemocatalytic production of addends. As described previously, furfural, a dehydrogenation product from pentoses, can undergo decarbonylation to furan over K-doped Pd/Al_2O_3 in reported yields over 99%.[148] 1-butene can be produced through the tandem dehydration/hydrogenation of glucose to γ-valerolactone (GVL, 48% yield) followed by decarboxylation, which has been accomplished with yields >98%.[169,170] 1,3-

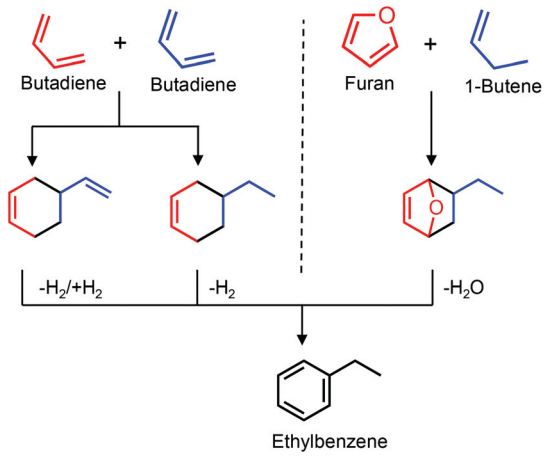

Fig. 16 Diels–Alder cycloaddition and subsequent dehydrogenative or dehydrative aromatization of biomass-derived addends for production of ethylbenzene.

Butadiene has been produced from ethanol over bifunctional mixed metal oxides in a pathway that involves the conversion of ethanol to acetaldehyde to acetaldol to crotonaldehyde and 3-hydroxybutanol to 1,3-butadiene. Using MgO-SiO_2, net 1,3-butadiene yields of 87% have been reported.[171]

Hybrid production of addends. Using engineered microorganisms, 1,3-butadiene can be synthesized through fermentation to produce 1,4-BDO and 2,3-BDO, followed by dehydration to 1,3-butadiene. A strain of *Escherichia coli* has been reported to produce 1,4-BDO at titers of >125 g L^{-1}, rates >3.5 g L^{-1} h^{-1}, and with biomass-derived hydrolyzate sugars.[172,173] Similarly, *Serratia marcescens* and *Klebsiella pneumoniae* have been reported to achieve 2,3-BDO titers of over 150 g L^{-1} at rates of up to 4.2 g L^{-1} h^{-1} with glucose and sucrose feedstocks, respectively.[174,175] 1,3-butadiene may be produced from either 1,4-BDO or 2,3-BDO through full dehydration, although more extensive studies have been reported for 2,3-BDO dehydrations, with reports of up to 88% 1,3-butadiene yield *via* dehydration over Sc_2O_3.[176]

Benzoic acid

Benzoic acid, commonly used as a food preservative and a precursor to polyesters and liquid crystal polymers, is an oxygen-containing commodity aromatic compound. In 2013, the global consumption of benzoic acid was nearly 500 000 metric tons, with a projected growth to just under 600 000 metric tons by 2018.[177] Commercial production of benzoic acid requires partial oxidation of toluene after separation from the products of catalytic petroleum reforming.[178] As described previously, this process first entails separation of high-purity toluene from petroleum reformate by liquid–liquid extraction. Following the isolation of toluene, a liquid-phase air oxidation to benzoic acid takes place, typically with the assistance of a cobalt or manganese-based catalyst.[135]

Diels–Alder production of biobased benzoic acid. Bio-derived furan can undergo Diels–Alder cycloaddition with bio-acrylic acid or methyl acrylate followed by dehydration for pro-

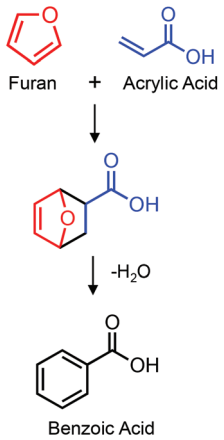

Fig. 17 Diels–Alder cycloaddition and subsequent dehydrative aromatization of biomass-derived addends for production of benzoic acid.

duction of benzoic acid or methyl benzoate (Fig. 17). The Diels–Alder reaction of furan with acrylic acid catalyzed by Lewis acid-modified Beta zeolites was reported at 51% cycloadduct yield with the subsequent dehydrative aromatization reaching benzoic acid yields of 43% when catalyzed by methanesulfonic acid. In contrast, the Diels–Alder cycloaddition of furan with methyl acrylate was reported with a yield of only 25%, but the yield of the subsequent dehydration was 96% using the same catalytic system as in the reaction of furan with acrylic acid. Both reactions were performed at low temperatures (25–60 °C) and ambient pressure under a nitrogen atmosphere.[179] In a computational study of this system, the zeotypic Lewis acids were shown to decrease the activation barrier for the Diels–Alder addition of furan with methyl acrylate from over 18 kcal mol^{-1} to *ca.* 2 kcal mol^{-1}.[180]

Chemocatalytic production of addends. For use in this reaction pathway, furan can be produced from biomass through the decarbonylation of furfural, as described previously. The chemocatalytic route of acrylic acid production from lignocellulosic biomass first involves conversion of cellulose to lactic acid, which was reported in yields up to 68% using a lead-based catalyst.[181] Lactic acid can undergo dehydration to acrylic acid over a base treated ZSM-5 catalyst to achieve 75% yield of acrylic acid.[182] An alternative chemocatalytic route of acrylic acid production involves the oxidation of glycerol. This pathway was recently reported using vanadium-substituted cesium salts of Keggin-type HPAs to achieve acrylic acid yields of up to 60%.[183]

Hybrid production of addends. Acrylic acid can also be produced from the fermentation of glucose to lactic acid by *Bacillus subtilis* in titers of up to 183 g L^{-1}.[184] Lactic acid is then dehydrated to acrylic acid over ZSM-5 as described above. Similarly, acrylic acid can be produced from the dehydration of 3-hydropropionic acid, the latter which has been extensively pursued by using engineered microorganisms with sugar feedstocks.[185]

Phthalic anhydride

The global consumption of phthalic anhydride, which has applications as an intermediate in the production of plasticizers, resins, and dyes, was estimated to be nearly 4 million metric tons in 2014 and is expected to grow to just under 4.5 million metric tons by 2019.[186] Traditionally, phthalic anhydride is prepared by the catalytic oxidation of *o*-xylene or naphthalene. Over time, *o*-xylene has become the dominant source for phthalic anhydride production due to greater availability and increased atom economy when compared to naphthalene. There are two general modes of commercial-scale *o*-xylene oxidation to phthalic anhydride: gas-phase or liquid-phase oxidation. However, the gas-phase oxidation with V_2O_5 based catalysts is the leading process and can achieve selectivity of up to 78%. Post-oxidation distillation results in nearly 100% pure phthalic anhydride.[135]

Diels–Alder production of biobased phthalic anhydride. Phthalic anhydride has been produced through the Diels–Alder cycloaddition of furan and maleic anhydride (Fig. 18), with reported cycloadduct yields of 96% after 4 h of reaction at room temperature and solvent free conditions, followed by dehydration in methanesulfonic acid at 80 °C for 4 h to achieve 80% net yield of phthalic anhydride.[82]

Chemocatalytic production of addends. The production of furan has been achieved from furfural in high yields as described previously. Maleic anhydride can be produced in 73% yield from furfural through selective oxidation over vanadia-alumina catalysts.[187] Additionally, maleic anhydride can be prepared *via* oxidation of biomass-derived levulinic acid using catalysts such as vanadia-alumina. Levulinic acid can be produced through decomposition of lignocellulosic sugars or bagasse, using mineral acid catalysts at reported yields of over 80%.[145,188]

Terephthalic acid

Terephthalic acid (TPA) and dimethyl terephthalate (DMTPA) are chiefly utilized for the production of polyethylene terephthalate (PET), which has experienced large market growth over the past years due to the large demand in the bottling

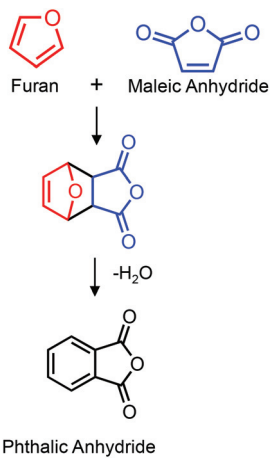

Fig. 18 Diels–Alder cycloaddition and subsequent dehydrative aromatization of biomass-derived addends for production of phthalic anhydride.

industry. Combined, the global consumption of TPA and DMTPA in 2013 was over 50 million metric tons, and is projected to grow to nearly 67 million metric tons by 2018.[189] Industrially, TPA and DMTPA are produced by the Witten process, which begins with *p*-xylene, extracted and isolated as described previously. *p*-Xylene then undergoes a two-stage liquid-phase oxidation, leading to a recovery of 88–90% of the theoretical yield.[135]

Diels–Alder production of biobased terephthalic acid. Of the existing routes for the production of biomass-derived TPA/DMTPA using Diels–Alder reactions, one route involves Diels–Alder addition and aromatization to produce *p*-xylene, followed by two-step oxidations to yield TPA. By first synthesizing *p*-xylene from biomass, thus necessitating a subsequent oxidation, the opportunity for an oxygen-retaining Diels–Alder process is lost. In contrast, the Diels–Alder reaction of bio-derived *trans*,*trans*-dimethyl muconate or oxidized variants of 5-HMF with ethylene to produce TPA/DMTPA utilizes oxygen retained in the addends (Fig. 19).[43,114] Recently, nearly 100% yield of the cycloadduct from the Diels–Alder addition of *trans*, *trans*-diethylmuconate and ethylene was reported using silicotungstate as the catalyst under reaction conditions of 200 °C, 30 bar ethylene, and reaction length of 4–6 h.[114] Overall yields to diethyl terephthalate of 80% were reported after palladium-catalyzed dehydrogenation of the cycloadduct under 1 bar of nitrogen at 200 °C for 6 h.

Similarly, the synthesis of TPA and DMTPA using partially oxidized variants of 5-HMF as the diene for Diels–Alder addition with ethylene has been proposed in literature.[43] The partial oxidation product of 5-HMF, 5-(hydroxymethyl)furoic acid (HMFA), and the methyl ester derivatives can be produced at near quantitative yield from 5-HMF. Subsequently, the reactions with ethylene were performed in batch at 190 °C and 37 bar using Sn-Beta zeolite catalyst. Cycloadduct yield of 19% was reported for the Diels–Alder reaction with HMFA and ethylene. Similarly, cycloadduct yield of 24% was reported for the addition of the methyl derivative of HMFA and ethylene. While direct dehydration of these Diels–Alder products has not yet been demonstrated, the resulting aromatic product is not terephthalic acid or dimethyl terephthalate, but rather a very similarly structured compound. A second, post Diels–Alder oxidation prior to dehydrative aromatization is necessary for targeting terephthalic acid/ester as the final product, though this reaction scheme was not reported.

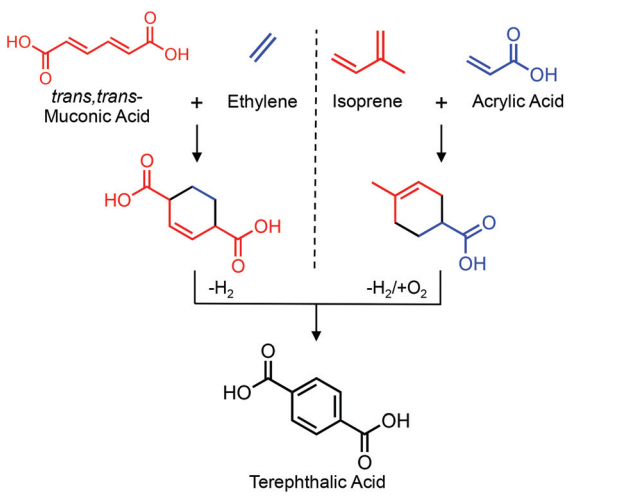

Fig. 19 Cycloaddition and subsequent dehydrogenative aromatization of biomass-derived addends in two representative routes of Diels–Alder based terephthalic acid production.

Another alternate route for terephthalic acid production involves the Diels–Alder cycloaddition of isoprene and acrylic acid, followed by dehydrogenative aromatization and oxidation.[190] The Diels–Alder reaction of isoprene with acrylic acid was reported at yields of up to 94% under solvent-free conditions using $TiCl_4$ at room temperature and 1 bar Ar after 24 h of reaction. Subsequently, Pd/C catalyzed aromatization *via* distillation of the cycloadduct at 240 °C and 0.11 bar Ar afforded 77% yield of *p*-toluic acid. Finally, oxidation using $Co(OAc)_2/Mn(OAc)_2$ in acetic acid under 1 atm O_2 at 100 °C afforded up to 94% yield of terephthalic acid.

Chemocatalytic production of addends. Utilizing oxidized variants of 5-HMF as the diene allows for a strictly chemocatalytic route, in which 5-HMF is first oxidized to a series of products that undergo Diels–Alder reactions with ethylene and a second oxygenation for production of terephthalic acid or dimethyl terephthalate. Yields of up to 24% have been reported for the Diels–Alder additions with subsequent dehydration of oxygenated variants of HMF with ethylene using Sn-Beta catalyst.[43] Yields for the oxidation to TPA or DMTPA have not been reported. As described for *p*-xylene production, 5-HMF may be directly produced from biomass using chromium chloride based catalysts. 5-HMF may then be partially oxidized over gold nanoparticles (NPs) to produce HMFA and ester derivatives of HMFA in nearly quantitative yields.[191]

Hybrid production of addends. *cis*,*cis*-Muconic acid can be produced through biological transformation of lignocellulosic biomass components (both sugars and lignin-derived aromatics) in titers of over 44 g L^{-1}.[192–194] In order to be functional in Diels–Alder cycloadditions, isomerization to *trans*, *trans*-muconic acid is necessary, and can be completed in over 80% yield using a molecular iodine catalyst.[195] After isomerization, *trans,trans*-muconic acid may be directly utilized in the Diels–Alder reaction with ethylene, or it can be esterified. The esterification to *trans,trans*-dimethyl muconate has been reported in 92% yield when catalyzed by sulfuric acid. Similarly, the esterification to *trans*,*trans*-diethyl muconate has been reported at >92% yield using sulfuric acid.[114]

Considerations with biomass feedstocks

As the catalytic routes for biomass valorization *via* Diels–Alder reactions advance, the challenge of utilizing complex lignocellulosic feedstocks will become increasingly important. The production of Diels–Alder addends from biomass can introduce a variety of challenges, including the carryover of non-target organics and inorganic contaminants that result from biomass feedstocks or during deconstruction and conversion

steps. This introduces demand for not only highly active and selective catalysts, but also for robust and stable catalyst materials.[196] Further, sufficient chemical purity is required for aromatic monomers used in commercial applications, necessitating the integration of separation methods to reduce energy requirements, materials, and cost. From a systems level perspective, early stage techno-economic and life cycle analysis can help guide the integration of unit operations and prioritize Diels–Alder routes for further development.[197–201] Often process economic gains and environmental impacts act in tension with one another,[202] highlighting the need for early stage systems modeling to inform sustainable process design. To ultimately commercialize direct replacement Diels–Alder aromatic monomers, companies will need to address the challenge of validating end-use applications, acquiring regulatory approval, establishing supply chain networks, and gaining consumer adoption. However, growing interest from both consumers and companies for developing biobased products with smaller environmental footprints can help provide market incentives for overcoming these barriers.

Functional alternatives

In addition to producing direct replacement commodity aromatics *via* Diels–Alder chemistry, the diversity of Diels–Alder addends that can be derived from biomass offers the potential for targeting novel aromatic monomers with unique structural, chemical, and functional properties (Fig. 20).[47,203] These unique monomer attributes can potentially lead to functional alternatives that exhibit unconventional properties for existing applications or that enable new end-use applications, in turn creating new market opportunities for biobased aromatics that would be difficult to access with petroleum-derived monomers.

Biological and chemocatalytic approaches, or a combination thereof, offer an incredible number of new routes from lignocellulosic biomass to novel or unexplored Diels–Alder addends. Biologically, addends possessing diverse functionalities may be produced *via* central carbon metabolism as well as through secondary metabolic pathways such as fatty acid, isoprenoid, and polyketide synthesis.[35] While utilizing targeted metabolic diversity as a means to access unique Diels–Alder addends is a relatively unexplored area, the ability to identify new addend candidates will be accelerated by combining emerging metabolic pathway databases[204] with efficient computational tools that enable chemical operators to be mapped in a targeted manner.[205] Extending this approach to include reaction networks that widen the scope to hybrid biological and chemocatalytic approaches will undoubtedly expand the diversity of Diels–Alder products that are accessible from lignocellulosic biomass building blocks.

With regards to polymer applications, Diels–Alder chemistry can be used to tailor monomer composition by a variety of approaches that include: (i) altering the branching of monomer pendant functional groups, (ii) introducing monomer molecular asymmetry, and (iii) tailoring monomer pendant group chemical speciation.

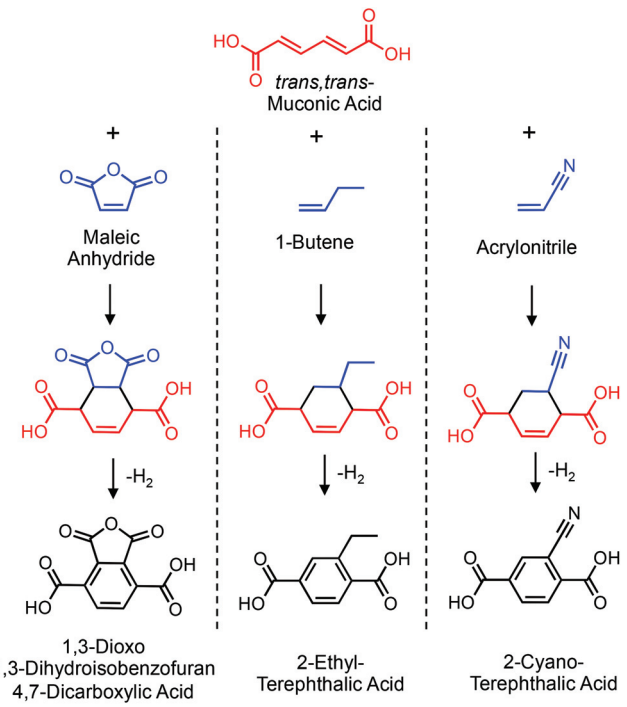

Fig. 20 Diels–Alder cycloaddition for the production of structurally unique aromatic monomers derived from *trans,trans*-muconic acid.

The synthesis of branched monomers *via* Diels–Alder chemistry will enable polymers that exhibit strain hardening during extensional processing flows, as well as enhanced biodegradability. Strain hardening is known to occur during the processing of branched polyethylene *via* blow molding and ultimately enables the large scale production of plastic bags.[206] Rheological control is paramount in processing polymer melts, and is necessary to enable the widespread implementation of biobased materials. With regards to biodegradability, a considerable amount of research has been conducted to introduce branching in polylactic acid to increase accessibility and promote hydrolysis of polyester bonds.[207] Branched polyesters can be achieved by incorporating multi-pendant group monomers during synthesis that possess three or more carboxylic acid groups. Such monomer functionality can be readily accessed from the Diels–Alder reaction of maleic anhydride and muconic acid,[195] which results in two carboxylic acid pendant groups and two additional carbonyl pendant groups (Fig. 20, left).

While branching in the polymer backbone can influence the rheological processing and biodegradability of polymers, asymmetrical monomer structures can facilitate amorphous polymers that are well suited for resin and composite applications. Recently, isophthalic acid was produced *via* the Diels–Alder reaction of 2-pyrone-4,6-dicarboxylic acid, a Diels–Alder addend derived from aromatic catabolic pathways, with ethylene.[208] Isophthalic acid is one of the primary components in

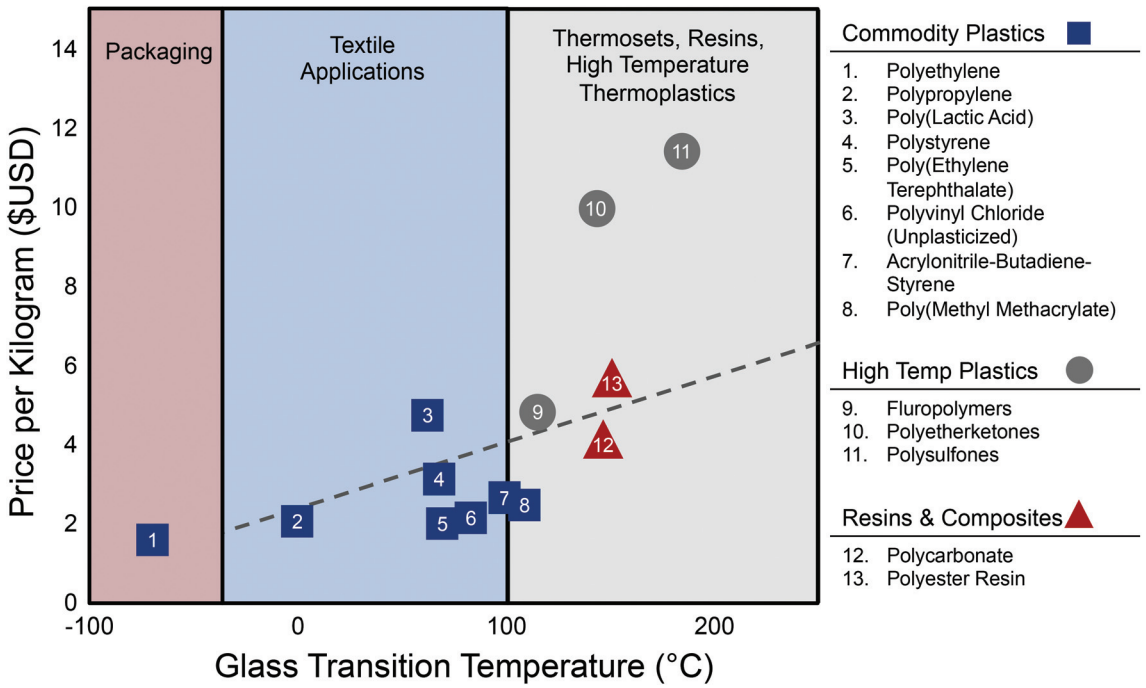

Fig. 21 Price per kilogram as a function of glass transition temperature for commodity plastics, high temperature plastics, and resin and composite materials.[211,212]

unsaturated polyesters because it disrupts the order of the polymer melt (when compared to terephthalic acid) and promotes high solubility of unsaturated polyesters in styrene. Aromatic monomer asymmetry is readily accessible *via* Diels–Alder chemistry through use of asymmetrical addends, as illustrated with the cycloaddition of 1-butene and muconic acid (Fig. 20, middle). The extent of disruption can be further tailored through the selective choice of addends (*e.g.*, 1-butene or longer chain alkene)[209,210] to enable a wide range of monomer asymmetries while maintaining the rigidity provided by the main aromatic structural unit.

Lastly, control of monomer pendant group chemical functionality can influence multiple polymer properties such as rigidity, crystallinity, chemical inertness, fire resistance, conductivity, gas permeability, and conductivity. Chemical functionality can be achieved with heteroatom pendant groups that contain fluorine, phosphorous, bromine, nitrogen, sulfur, or other elements of interest. Often, due to their enhanced performance, functionalized polymers can command a much higher price compared to less-functionalized commodity plastics (Fig. 21). Heteroatom functionalities have known effects on polymer performance and Diels–Alder chemistry offers a highly regioselective manner for the incorporation of heteroatoms into biobased aromatic monomers in an effort to target particular performance attributes. For example, the Diels–Alder cycloaddition of acrylonitrile with muconic acid can introduce a nitrile pendant group that may be capable of increasing polymer rigidity and solvent barrier properties (Fig. 20, right). Although the utility of such functional groups would need to be further explored, commercial market opportunities are likely if biobased Diels–Alder products can achieve performance-differentiating attributes in a cost-competitive fashion.

While not exhaustive, the functional alternative monomers described above highlight the wide degree of chemical control and specificity available *via* Diels–Alder reactions. In addition, although not covered in this review, catalyzed Diels–Alder chemistry affords cycloadduct stereochemical control that may enable new chiral materials and innovative end-use applications.[213] These can include advanced materials, specialty chemicals, agricultural products, and human health products. Moving forward, advances in metabolic engineering and tailored chemocatalysis will continue to generate new biobased Diels–Alder addends and cycloadducts that provide exciting opportunities for further research. Novel end-use applications can be further refined and ideally determine *a priori* through an improved understanding of structure–function relationships gained *via* computational, high-throughput testing, and informatics approaches.

Conclusion

As discussed in this review, Diels–Alder cycloadditions offer a promising route for the production of both commercial direct replacement and functional alternative aromatic monomers. With ongoing investigations into the conversion of biomass into Diels–Alder addends and the design of multifunctional catalyst materials to enable tandem cycloaddition and aromatization reactions, the production of biomass-derived aromatic

monomers will continue to become more efficient. High-yielding Diels–Alder conversion routes are now transitioning from model compounds studies to complex lignocellulosic biomass to avoid competition with food resources and lower feedstock costs. Finally, the development of functional alternative aromatic monomers *via* Diels–Alder chemistry may afford new end-use applications that provide market-driven incentives to advance biomass conversion technologies.

Acknowledgements

We would like to thank the U.S. Department of Energy Bioenergy Technologies Office for funding this work *via* Contract No. DE-AC36-08GO28308 at the National Renewable Energy Laboratory. NAR and GTB also partially thank the Laboratory Directed Research and Development (LDRD) program at the National Renewable Energy Laboratory for partial funding for this effort. Lastly, DRV and GTB thank the Direct Catalytic Conversion of Biomass to Biofuels (C3Bio), an Energy Frontier Research Center funded by the U.S. Department of Energy, Office of Science, Office of Basic Energy Sciences, Award Number DE-SC0000997. We would like to thank Dr Seonah Kim for insightful discussions regarding this manuscript and help with zeolite figure modeling.

References

1 V. Teske and C. Willett, *IHS Chemical Chemical Economics Handbook - PET Polymer*, 2015.
2 D. I. Collias, A. M. Harris, V. Nagpal, I. W. Cottrell and M. W. Schultheis, Biobased Terephthalic Acid Technologies: A Literature Review, *Ind. Biotechnol.*, 2014, **10**, 91–105.
3 A. Maneffa, P. Priecel and J. A. Lopez-Sanchez, Biomass-Derived Renewable Aromatics: Selective Routes and Outlook for p-Xylene Commercialisation, *ChemSusChem*, 2016, **9**, 2736–2748.
4 A. M. Niziolek, O. Onel, Y. A. Guzman and C. A. Floudas, Biomass-Based Production of Benzene, Toluene, and Xylenes via Methanol: Process Synthesis and Deterministic Global Optimization, *Energy Fuels*, 2016, **30**, 4970–4998.
5 G. W. Huber, S. Iborra and A. Corma, Synthesis of Transportation Fuels from Biomass: Chemistry, Catalysts, and Engineering, *Chem. Rev.*, 2006, **106**, 4044–4098.
6 R. A. Sheldon, Green and sustainable manufacture of chemicals from biomass: state of the art, *Green Chem.*, 2014, **16**, 950–963.
7 I. Delidovich, *et al.* Alternative Monomers Based on Lignocellulose and Their Use for Polymer Production, *Chem. Rev.*, 2016, **116**, 1540–1599.
8 Y. Zhu, C. Romain and C. K. Williams, Sustainable polymers from renewable resources, *Nature*, 2016, **540**, 354–362.
9 T. Damartzis and A. Zabaniotou, Thermochemical conversion of biomass to second generation biofuels through integrated process design—A review, *Renewable Sustainable Energy Rev.*, 2011, **15**, 366–378.
10 J. Zakzeski, P. C. Bruijnincx, A. L. Jongerius and B. M. Weckhuysen, The catalytic valorization of lignin for the production of renewable chemicals, *Chem. Rev.*, 2010, **110**, 3552–3599.
11 A. V. Bridgwater, Review of fast pyrolysis of biomass and product upgrading, *Biomass Bioenergy*, 2012, **38**, 68–94.
12 C. A. Mullen and A. Boateng, A. Chemical Composition of Bio-oils Produced by Fast Pyrolysis of Two Energy Crops, *Energy Fuels*, 2008, **22**, 2104–2109.
13 D. C. Elliott, T. R. Hart, G. G. Neuenschwander, L. J. Rotness and A. H. Zacher, Catalytic hydroprocessing of biomass fast pyrolysis bio oil to produce hydrocarbon products, *Environ. Prog. Sustainable Energy*, 2009, **28**, 441–449.
14 T. P. Vispute, H. Zhang, A. Sanna, R. Xiao and G. W. Huber, Renewable chemical commodity feedstocks from integrated catalytic processing of pyrolysis oils, *Science*, 2010, **330**, 1222–1227.
15 A. H. Zacher, M. V. Olarte, D. M. Santosa, D. C. Elliott and S. B. Jones, A review and perspective of recent bio-oil hydrotreating research, *Green Chem.*, 2014, **16**, 491–515.
16 T. Carlson, Y.-T. Cheng, J. Jae and G. W. Huber, Production of green aromatics and olefins by catalytic fast pyrolysis of wood sawdust, *Energy Environ. Sci.*, 2011, **4**, 145–161.
17 C. Liu, H. Wang, M. A. Karim, J. Sun and Y. Wang, Catalytic fast pyrolysis of lignocellulosic biomass, *Chem. Soc. Rev.*, 2014, **43**, 7594–7623.
18 Anellotech, Inc., *Anellotech, Inc.*, available at: http://anellotech.com/ (accessed: 29th January 2017).
19 G. W. Huber, A. M. Gaffney, J. Jae and Y.-T. Cheng, *Systems and processes for catalytic pyrolysis of biomass and hydrocarbonaceous materials for production of aromatics with optional olefin recycle, and catalysts having selected particle size for catalytic pyrolysis*, 2012.
20 D. Sutton, B. Kelleher and J. R. H. Ross, Review of literature on catalysts for biomass gasification, *Fuel Process. Technol.*, 2001, **73**, 155–173.
21 E. van Steen and M. Claeys, Fischer-Tropsch Catalysts for the Biomass-to-Liquid (BTL)-Process, *Chem. Eng. Technol.*, 2008, **31**, 655–666.
22 R. Rauch, J. Hrbek and H. Hofbauer, Biomass gasification for synthesis gas production and applications of the syngas, *Wiley Interdiscip. Rev.: Energy Environ.*, 2014, **3**, 343–362.
23 X. Chen, *et al.*, DMR (deacetylation and mechanical refining) processing of corn stover achieves high monomeric sugar concentrations (230 g L^{-1}) during enzymatic hydrolysis and high ethanol concentrations (>10% v/v) during fermentation without hydrolysate purification or concentration, *Energy Environ. Sci.*, 2016, **9**, 1237–1245.

24 J. S. Luterbacher, *et al.*, Nonenzymatic Sugar Production from Biomass Using Biomass-Derived γ-Valerolactone, *Science*, 2014, **343**, 277–280.
25 Y. Sun and J. Cheng, Hydrolysis of lignocellulosic materials for ethanol production: a review, *Bioresour. Technol.*, 2002, **83**, 1–11.
26 B. Yang and C. E. Wyman, Pretreatment: the key to unlocking low-cost cellulosic ethanol, *Biofuels, Bioprod. Biorefin.*, 2008, **2**, 26–40.
27 G. T. Beckham, C. W. Johnson, E. M. Karp, D. Salvachúa and D. R. Vardon, Opportunities and challenges in biological lignin valorization, *Curr. Opin. Biotechnol.*, 2016, **42**, 40–53.
28 A. J. Ragauskas, *et al.*, The Path Forward for Biofuels and Biomaterials, *Science*, 2006, **311**, 484–489.
29 S. P. S. Chundawat, G. T. Beckham, M. E. Himmel and B. E. Dale, Deconstruction of Lignocellulosic Biomass to Fuels and Chemicals, *Annu. Rev. Chem. Biomol. Eng.*, 2011, **2**, 121–145.
30 M. E. Himmel, *et al.*, Biomass Recalcitrance: Engineering Plants and Enzymes for Biofuels Production, *Science*, 2007, **315**, 804–807.
31 T. J. Schwartz, B. H. Shanks and J. A. Dumesic, Coupling chemical and biological catalysis: a flexible paradigm for producing biobased chemicals, *Curr. Opin. Biotechnol.*, 2016, **38**, 54–62.
32 A. Galadima and O. Muraza, Zeolite catalysts in upgrading of bioethanol to fuels range hydrocarbons: A review, *J. Ind. Eng. Chem.*, 2015, **31**, 1–14.
33 J. Sun and Y. Wang, Recent Advances in Catalytic Conversion of Ethanol to Chemicals, *ACS Catal.*, 2014, **4**, 1078–1090.
34 Vertimass completes scale-up technology validation with DOE | Biomassmagazine.com. Available at: http://biomassmagazine.com/articles/12516/vertimass-completes-scale-up-technology-validation-with-doe (accessed: 29th January 2017).
35 P. P. Peralta-Yahya, F. Zhang, S. B. del Cardayre and J. D. Keasling, Microbial engineering for the production of advanced biofuels, *Nature*, 2012, **488**, 320–328.
36 J. J. Minty, *et al.*, Design and characterization of synthetic fungal-bacterial consortia for direct production of isobutanol from cellulosic biomass, *Proc. Natl. Acad. Sci. U. S. A.*, 2013, **110**, 14592–14597.
37 Gevo, Inc., *Gevo Inc.*, available at: http://gevo.com/ (accessed: 29th January 2017).
38 M. W. Peters, J. D. Taylor, M. Jenni, L. E. Manzer and D. E. Henton, *Integrated Process to Selectively Convert Renewable Isobutanol to P-Xylene*, 2011.
39 R. D. Cortright and P. G. Blommel, *Synthesis of liquid fuels and chemicals from oxygenated hydrocarbons*, 2013.
40 Virent, Inc., *Virent, Inc.*, Available at: http://www.virent.com/ (accessed: 29th January 2017).
41 R. Davis, *et al.*, Process design and economics for the conversion of lignocellulosic biomass to hydrocarbons: Dilute-acid and enzymatic deconstruction of biomass to sugars and catalytic conversion of sugars to hydrocarbons, *NREL Tech. Rep.*, 2015, 29–42.
42 H. J. Cho, *et al.*, Renewable p-Xylene from 2,5-Dimethylfuran and Ethylene Using Phosphorus-Containing Zeolite Catalysts, *ChemCatChem*, 2017, 398–402.
43 J. J. Pacheco and M. E. Davis, Synthesis of terephthalic acid via Diels-Alder reactions with ethylene and oxidized variants of 5-hydroxymethylfurfural, *Proc. Natl. Acad. Sci. U. S. A.*, 2014, **111**, 8363–8367.
44 C. L. Williams, *et al.*, Cycloaddition of biomass-derived furans for catalytic production of renewable p-xylene, *ACS Catal.*, 2012, **2**, 935–939.
45 C.-C. Chang, *et al.*, Lewis acid zeolites for tandem Diels–Alder cycloaddition and dehydration of biomass-derived dimethylfuran and ethylene to renewable p-xylene, *Green Chem.*, 2016, **18**, 1368–1376.
46 J.-L. Sánchez-García, R. García-Alamilla, M. M. González-Chávez, B. E. Handy and M.-G. Cárdenas-Galindo, Dehydrogenation and Diels–Alder reactions in a one-pot synthesis of benzaldehyde from n-butane over acid catalysts, *Catal. Commun.*, 2012, **27**, 154–158.
47 B. Shanks and P. Keeling, Bioprivileged molecules: creating value from biomass, *Green Chem.*, 2017, DOI: 10.1039/C7GC00296C.
48 N. A. Rorrer, *et al.*, Renewable Unsaturated Polyesters from Muconic Acid, *ACS Sustainable Chem. Eng.*, 2016, **4**, 6867–6876.
49 N. A. Rorrer, D. R. Vardon, J. R. Dorgan, E. J. Gjersing and G. T. Beckham, Biomass-derived monomers for performance-differentiated fiber reinforced polymer composites, *Green Chem.*, 2017, DOI: 10.1039/C7GC00320J.
50 J.-A. Funel and S. Abele, Industrial Applications of the Diels–Alder Reaction, *Angew. Chem., Int. Ed.*, 2013, **52**, 3822–3863.
51 K. N. Houk, Y. T. Lin and F. K. Brown, Evidence for the concerted mechanism of the Diels-Alder reaction of butadiene with ethylene, *J. Am. Chem. Soc.*, 1986, **108**, 554–556.
52 R. B. Woodward and R. Hoffmann, The Conservation of Orbital Symmetry, *Angew. Chem., Int. Ed. Engl.*, 1969, **8**, 781–853.
53 M. Linder and T. Brinck, Stepwise Diels–Alder: More than Just an Oddity? A Computational Mechanistic Study, *J. Org. Chem.*, 2012, **77**, 6563–6573.
54 E. Goldstein, B. Beno and K. N. Houk, Density Functional Theory Prediction of the Relative Energies and Isotope Effects for the Concerted and Stepwise Mechanisms of the Diels–Alder Reaction of Butadiene and Ethylene, *J. Am. Chem. Soc.*, 1996, **118**, 6036–6043.
55 F. Fringuelli and A. Taticchi, *The Diels-Alder Reaction: Selected Practical Methods*, John Wiley & Sons, 2002.
56 S. Noorizadeh and H. Maihami, A theoretical study on the regioselectivity of Diels–Alder reactions using electrophilicity index, *J. Mol. Struct. (THEOCHEM)*, 2006, **763**, 133–144.

57 Y. Xia, *et al.*, Impact of Lewis Acids on Diels–Alder Reaction Reactivity: A Conceptual Density Functional Theory Study, *J. Phys. Chem. A*, 2008, **112**, 9970–9977.
58 R. Hoffmann and R. B. Woodward, Orbital Symmetries and endo-exo Relationships in Concerted Cycloaddition Reactions, *J. Am. Chem. Soc.*, 1965, **87**, 4388–4389.
59 J. Sauer and R. Sustmann, Mechanistic Aspects of Diels-Alder Reactions: A Critical Survey, *Angew. Chem., Int. Ed. Engl.*, 1980, **19**, 779–807.
60 M. Yoshizawa, M. Tamura and M. Fujita, Diels-Alder in Aqueous Molecular Hosts: Unusual Regioselectivity and Efficient Catalysis, *Science*, 2006, **312**, 251–254.
61 H. Yamamoto and K. Futatsugi, 'Designer Acids': Combined Acid Catalysis for Asymmetric Synthesis, *Angew. Chem., Int. Ed.*, 2005, **44**, 1924–1942.
62 O. Diels and K. Alder, Synthesen in der hydroaromatischen Reihe, *Justus Liebigs Ann. Chem.*, 1928, **460**, 98–122.
63 A. Wassermann, Homogeneous catalysis of diene syntheses. A new type of third-order reaction, *J. Chem. Soc.*, 1942, 618–621.
64 P. Yates and P. Eaton, Acceleration of the Diels-Alder reaction by aluminum chloride, *J. Am. Chem. Soc.*, 1960, **82**, 4436–4437.
65 K. N. Houk, Frontier molecular orbital theory of cycloaddition reactions, *Acc. Chem. Res.*, 1975, **8**, 361–369.
66 N. Nikbin, *et al.*, A DFT study of the acid-catalyzed conversion of 2,5-dimethylfuran and ethylene to p-xylene, *J. Catal.*, 2013, **297**, 35–43.
67 D. H. Ess, G. O. Jones and K. N. Houk, Conceptual, Qualitative, and Quantitative Theories of 1,3-Dipolar and Diels–Alder Cycloadditions Used in Synthesis, *Adv. Synth. Catal.*, 2006, **348**, 2337–2361.
68 L. C. Dias, Chiral Lewis acid catalysts in diels-Alder cycloadditions: mechanistic aspects and synthetic applications of recent systems, *J. Braz. Chem. Soc.*, 1997, **8**, 289–332.
69 J. I. García, V. Martínez-Merino, J. A. Mayoral and L. Salvatella, Density Functional Theory Study of a Lewis Acid Catalyzed Diels–Alder Reaction. The Butadiene+Acrolein Paradigm, *J. Am. Chem. Soc.*, 1998, **120**, 2415–2420.
70 D. M. Birney and K. N. Houk, Transition structures of the Lewis acid-catalyzed Diels-Alder reaction of butadiene with acrolein. The origins of selectivity, *J. Am. Chem. Soc.*, 1990, **112**, 4127–4133.
71 M. Tao, *et al.*, Tailoring the Synergistic Bronsted-Lewis acidic effects in Heteropolyacid catalysts: Applied in Esterification and Transesterification Reactions, *Sci. Rep.*, 2015, **5**, 13764.
72 S. Telalović, *et al.*, Synergy between Brønsted acid sites and Lewis acid sites, *Chem. Commun.*, 2008, 4631–4633, DOI: 10.1039/B807953F.
73 S. Li, *et al.*, Probing the Spatial Proximities among Acid Sites in Dealuminated H-Y Zeolite by Solid-State NMR Spectroscopy, *J. Phys. Chem. C*, 2008, **112**, 14486–14494.
74 S. Li, *et al.*, Brønsted/Lewis Acid Synergy in Dealuminated HY Zeolite: A Combined Solid-State NMR and Theoretical Calculation Study, *J. Am. Chem. Soc.*, 2007, **129**, 11161–11171.
75 Z. Wang, L. Wang, Y. Jiang, M. Hunger and J. Huang, Cooperativity of Brønsted and Lewis Acid Sites on Zeolite for Glycerol Dehydration, *ACS Catal.*, 2014, **4**, 1144–1147.
76 Z. Yu, *et al.*, Brønsted/Lewis Acid Synergy in H–ZSM-5 and H–MOR Zeolites Studied by 1H and 27Al DQ-MAS Solid-State NMR Spectroscopy, *J. Phys. Chem. C*, 2011, **115**, 22320–22327.
77 A. Zheng, S. Li, S.-B. Liu and F. Deng, Acidic Properties and Structure–Activity Correlations of Solid Acid Catalysts Revealed by Solid-State NMR Spectroscopy, *Acc. Chem. Res.*, 2016, **49**, 655–663.
78 G. Kraus, G. R. P. Iii, C. L. Beck, K. Palmer and A. H. Winter, Aromatics from pyrones: esters of terephthalic acid and isophthalic acid from methyl coumalate, *RSC Adv.*, 2013, **3**, 12721–12725.
79 J. Lee, G. R. P. Iii, D. Mitchell, L. Kasuga and G. A. Kraus, Upgrading malic acid to bio-based benzoates via a Diels–Alder-initiated sequence with the methyl coumalate platform, *RSC Adv.*, 2014, **4**, 45657–45664.
80 J. J. Lee and G. A. Kraus, One-pot formal synthesis of biorenewable terephthalic acid from methyl coumalate and methyl pyruvate, *Green Chem.*, 2014, **16**, 2111–2116.
81 M. Shiramizu and F. D. Toste, On the Diels–Alder approach to solely biomass-derived polyethylene terephthalate (PET): conversion of 2, 5-dimethylfuran and acrolein into p-xylene, *Chem. – Eur. J.*, 2011, **17**, 12452–12457.
82 E. Mahmoud, D. A. Watson and R. F. Lobo, Renewable production of phthalic anhydride from biomass-derived furan and maleic anhydride, *Green Chem.*, 2013, **16**, 167–175.
83 T. Salavati-fard, S. Caratzoulas and D. J. Doren, Solvent Effects in Acid-Catalyzed Dehydration of the Diels-Alder Cycloadduct between 2,5-Dimethylfuran and Maleic Anhydride, *Chem. Phys.*, 2017, 118–124.
84 R. Patet, W. Fan, D. G. Vlachos and S. Caratzoulas, Tandem Diels-Alder of Dimethylfuran and Ethylene and Dehydration to para-Xylene Catalyzed by Zeotypic Lewis Acids, *ChemCatChem*, 2017, DOI: 10.1002/cctc.201601584.
85 P. Kostestkyy, J. Yu, R. J. Gorte and G. Mpourmpakis, Structure–activity relationships on metal-oxides: alcohol dehydration, *Catal. Sci. Technol.*, 2014, **4**, 3861–3869.
86 J. J. H. B. Sattler, J. Ruiz-Martinez, E. Santillan-Jimenez and B. M. Weckhuysen, Catalytic Dehydrogenation of Light Alkanes on Metals and Metal Oxides, *Chem. Rev.*, 2014, **114**, 10613–10653.
87 J. A. Lercher, R. A. van Santen and H. Vinek, Carbonium ion formation in zeolite catalysis, *Catal. Lett.*, 1994, **27**, 91–96.
88 S. R. Blaszkowski, A. P. J. Jansen, M. A. C. Nascimento and R. A. Van Santen, Density Functional Theory Calculations of the Transition States for Hydrogen Exchange and

Dehydrogenation of Methane by a Broensted Zeolitic Proton, *J. Phys. Chem.*, 1994, **98**, 12938–12944.

89 V. B. Kazansky, M. V. Frash and R. A. van Santen, A quantum-chemical study of adsorbed nonclassical carbonium ions as active intermediates in catalytic transformations of paraffins. II. Protolytic dehydrogenation and hydrogen-deuterium hetero-isotope exchange of paraffins on high-silica zeolites, *Catal. Lett.*, 1994, **28**, 211–222.

90 L. Wang, *et al.*, Dehydrogenation and aromatization of methane under non-oxidizing conditions, *Catal. Lett.*, 1993, **21**, 35–41.

91 R. A. Sheldon and R. S. Downing, Heterogeneous catalytic transformations for environmentally friendly production, *Appl. Catal., A*, 1999, **189**, 163–183.

92 B. M. Weckhuysen and J. Yu, Recent advances in zeolite chemistry and catalysis, *Chem. Soc. Rev.*, 2015, **44**, 7022–7024.

93 M. Zaarour, B. Dong, I. Naydenova, R. Retoux and S. Mintova, Progress in zeolite synthesis promotes advanced applications, *Microporous Mesoporous Mater.*, 2014, **189**, 11–21.

94 M. Milina, S. Mitchell, N.-L. Michels, J. Kenvin and J. Pérez-Ramírez, Interdependence between porosity, acidity, and catalytic performance in hierarchical ZSM-5 zeolites prepared by post-synthetic modification, *J. Catal.*, 2013, **308**, 398–407.

95 E. F. Iliopoulou, *et al.*, Catalytic upgrading of biomass pyrolysis vapors using transition metal-modified ZSM-5 zeolite, *Appl. Catal., B*, 2012, **127**, 281–290.

96 N. Nikbin, S. Feng, S. Caratzoulas and D. G. Vlachos, p-Xylene Formation by Dehydrative Aromatization of a Diels–Alder Product in Lewis and Brønsted Acidic Zeolites, *J. Phys. Chem. C*, 2014, **118**, 24415–24424.

97 C.-C. Chang, S. K. Green, C. L. Williams, P. J. Dauenhauer and W. Fan, Ultra-selective cycloaddition of dimethylfuran for renewable p-xylene with H-BEA, *Green Chem.*, 2014, **16**, 585–588.

98 Y. P. Wijaya, D. J. Suh and J. Jae, Production of renewable p-xylene from 2,5-dimethylfuran via Diels–Alder cycloaddition and dehydrative aromatization reactions over silica–alumina aerogel catalysts, *Catal. Commun.*, 2015, **70**, 12–16.

99 J. M. R. Gallo, *et al.*, Production of Furfural from Lignocellulosic Biomass Using Beta Zeolite and Biomass-Derived Solvent, *Top. Catal.*, 2013, **56**, 1775–1781.

100 I. F. Teixeira, *et al.*, From Biomass-Derived Furans to Aromatics with Ethanol over Zeolite, *Angew. Chem., Int. Ed.*, 2016, **55**, 13061–13066.

101 Y. Cheng, *et al.*, Oxidative dehydrogenation of ethane with CO2 over Cr supported on submicron ZSM-5 zeolite, *Chin. J. Catal.*, 2015, **36**, 1242–1248.

102 R. B. Borade, B. Zhang and A. Clearfield, Selective dehydrogenation of cyclohexene to benzene using Pd-exchanged α-zirconium phosphate, *Catal. Lett.*, 1997, **45**, 233–235.

103 M. Lezanska, G. S. Szymanski, P. Pietrzyk, Z. Sojka and J. A. Lercher, Characterization of Cr–MCM-41 and Al, Cr–MCM-41 Mesoporous Catalysts for Gas-Phase Oxidative Dehydrogenation of Cyclohexane, *J. Phys. Chem. C*, 2007, **111**, 1830–1839.

104 A. M. Aliev, Z. A. Shabanova, U. M. Nadzhaf-Kuliev and S. M. Medzhidova, Oxidative dehydrogenation of cyclohexane over modified zeolite catalysts, *Pet. Chem.*, 2016, **56**, 639–645.

105 P. A. Weyrich and W. F. Hölderich, Dehydrogenation of α-limonene over Ce promoted, zeolite supported Pd catalysts, *Appl. Catal., A*, 1997, **158**, 145–162.

106 J. Zhang and C. Zhao, Development of a Bimetallic Pd-Ni/HZSM-5 Catalyst for the Tandem Limonene Dehydrogenation and Fatty Acid Deoxygenation to Alkanes and Arenes for Use as Biojet Fuel, *ACS Catal.*, 2016, **6**, 4512–4525.

107 R. B. Biniwale, N. Kariya and M. Ichikawa, Dehydrogenation of Cyclohexane Over Ni Based Catalysts Supported on Activated Carbon using Spray-pulsed Reactor and Enhancement in Activity by Addition of a Small Amount of Pt, *Catal. Lett.*, 2005, **105**, 83–87.

108 N. Mizuno, K. Yamaguchi and K. Kamata, Epoxidation of olefins with hydrogen peroxide catalyzed by polyoxometalates, *Coord. Chem. Rev.*, 2005, **249**, 1944–1956.

109 S.-S. Wang and G.-Y. Yang, Recent Advances in Polyoxometalate-Catalyzed Reactions, *Chem. Rev.*, 2015, **115**, 4893–4962.

110 D.-L. Long, E. Burkholder and L. Cronin, Polyoxometalate clusters, nanostructures and materials: From self assembly to designer materials and devices, *Chem. Soc. Rev.*, 2007, **36**, 105–121.

111 T. Okuhara, T. Nishimura, H. Watanabe and M. Misono, Insoluble heteropoly compounds as highly active catalysts for liquid-phase reactions, *J. Mol. Catal.*, 1992, **74**, 247–256.

112 I. V. Kozhevnikov, Catalysis by Heteropoly Acids and Multicomponent Polyoxometalates in Liquid-Phase Reactions, *Chem. Rev.*, 1998, **98**, 171–198.

113 I. V. Kozhevnikov, Sustainable heterogeneous acid catalysis by heteropoly acids, *J. Mol. Catal. A: Chem.*, 2007, **262**, 86–92.

114 R. Lu, *et al.*, Production of Diethyl Terephthalate from Biomass-Derived Muconic Acid, *Angew. Chem., Int. Ed.*, 2016, **128**, 257–261.

115 G. J. Meuzelaar, L. Maat, R. A. Sheldon and I. V. Kozhevnikov, Heteropoly acid-catalyzed Diels-Alder reactions, *Catal. Lett.*, 1997, **45**, 249–251.

116 V. V. Bokade and G. D. Yadav, Heteropolyacid supported on montmorillonite catalyst for dehydration of dilute bioethanol, *Appl. Clay Sci.*, 2011, **53**, 263–271.

117 Y. Zhang, V. Degirmenci, C. Li and E. J. M. Hensen, Phosphotungstic Acid Encapsulated in Metal–Organic Framework as Catalysts for Carbohydrate Dehydration to 5-Hydroxymethylfurfural, *ChemSusChem*, 2011, **4**, 59–64.

118 D. R. Park, *et al.*, Correlation between reduction potential of vanadium-containing heteropolyacid HPA catalysts and

their oxidation activity for cyclohexanol dehydrogenation, *React. Kinet. Catal. Lett.*, 2008, **93**, 43–49.
119 C. Spino, H. Rezaei and Y. L. Dory, Characteristics of the Two Frontier Orbital Interactions in the Diels–Alder Cycloaddition, *J. Org. Chem.*, 2004, **69**, 757–764.
120 H. Hirao and T. Ohwada, Theoretical Revisit of Regioselectivities of Diels–Alder Reactions: Orbital-Based Reevaluation of Multicentered Reactivity in Terms of Reactive Hybrid Orbitals, *J. Phys. Chem. A*, 2005, **109**, 816–824.
121 F. Liu, R. S. Paton, S. Kim, Y. Liang and K. N. Houk, Diels–Alder Reactivities of Strained and Unstrained Cycloalkenes with Normal and Inverse-Electron-Demand Dienes: Activation Barriers and Distortion/Interaction Analysis, *J. Am. Chem. Soc.*, 2013, **135**, 15642–15649.
122 R. S. Paton, S. Kim, A. G. Ross, S. J. Danishefsky and K. N. Houk, Experimental Diels–Alder Reactivities of Cycloalkenones and Cyclic Dienes Explained through Transition-State Distortion Energies, *Angew. Chem., Int. Ed.*, 2011, **50**, 10366–10368.
123 I. Fernández and F. M. Bickelhaupt, Deeper Insight into the Diels–Alder Reaction through the Activation Strain Model, *Chem. – Asian J.*, 2016, **11**, 3297–3304.
124 K. N. Houk and P. H.-Y. Cheong, Computational prediction of small-molecule catalysts, *Nature*, 2008, **455**, 309–313.
125 J. K. Nørskov, T. Bligaard, J. Rossmeisl and C. H. Christensen, Towards the computational design of solid catalysts, *Nat. Chem.*, 2009, **1**, 37–46.
126 P. H.-Y. Cheong, C. Y. Legault, J. M. Um, N. Çelebi-Ölçüm and K. N. Houk, Quantum Mechanical Investigations of Organocatalysis: Mechanisms, Reactivities, and Selectivities, *Chem. Rev.*, 2011, **111**, 5042–5137.
127 Y. Wang, *et al.*, A Computationally Designed Rh(I)-Catalyzed Two-Component [5+2+1] Cycloaddition of Ene-vinylcyclopropanes and CO for the Synthesis of Cyclooctenones, *J. Am. Chem. Soc.*, 2007, **129**, 10060–10061.
128 M. N. Paddon-Row, L. C. H. Kwan, A. C. Willis and M. S. Sherburn, Enantioselective Oxazaborolidinium-Catalyzed Diels–Alder Reactions without CH···O Hydrogen Bonding, *Angew. Chem., Int. Ed.*, 2008, **47**, 7013–7017.
129 M. N. Paddon-Row, C. D. Anderson and K. N. Houk, Computational Evaluation of Enantioselective Diels–Alder Reactions Mediated by Corey's Cationic Oxazaborolidine Catalysts, *J. Org. Chem.*, 2009, **74**, 861–868.
130 W. Liao and Z.-X. Yu, DFT Study of the Mechanism and Stereochemistry of the Rh(I)-Catalyzed Diels–Alder Reactions between Electronically Neutral Dienes and Dienophiles, *J. Org. Chem.*, 2014, **79**, 11949–11960.
131 R. E. Patet, *et al.*, Kinetic Regime Change in the Tandem Dehydrative Aromatization of Furan Diels–Alder Products, *ACS Catal.*, 2015, **5**, 2367–2375.
132 Y.-P. Li, M. Head-Gordon and A. T. Bell, Computational Study of p-Xylene Synthesis from Ethylene and 2,5-Dimethylfuran Catalyzed by H-BEA, *J. Phys. Chem. C*, 2014, **118**, 22090–22095.
133 S. Van de Vyver and Y. Román-Leshkov, Metalloenzyme-Like Zeolites as Lewis Acid Catalysts for C-C Bond Formation, *Angew. Chem., Int. Ed.*, 2015, **54**, 12554–12561.
134 X. López, J. J. Carbó, C. Bo and J. M. Poblet, Structure, properties and reactivity of polyoxometalates: a theoretical perspective, *Chem. Soc. Rev.*, 2012, **41**, 7537–7571.
135 K. Weissermel and H.-J. Arpe, *Industrial Organic Chemistry*, John Wiley & Sons, 2003.
136 H. Chen, *Lignocellulose Biorefinery Engineering: Principles and Applications*, Woodhead Publishing, 2015.
137 M. Dusselier, M. Mascal and B. F. Sels, *Top Chemical Opportunities from Carbohydrate Biomass: A Chemist's View of the Biorefinery*, Springer Berlin Heidelberg, 2014, pp. 1–40.
138 M. Montazeri, G. G. Zaimes, V. Khanna and M. J. Eckelman, Meta-Analysis of Life Cycle Energy and Greenhouse Gas Emissions for Priority Biobased Chemicals, *ACS Sustainable Chem. Eng.*, 2016, **4**, 6443–6454.
139 J. E. Matthiesen, *et al.*, Electrochemical Conversion of Biologically Produced Muconic Acid: Key Considerations for Scale-Up and Corresponding Technoeconomic Analysis, *ACS Sustainable Chem. Eng.*, 2016, **4**, 7098–7109.
140 K. Smith and P. Feng, *IHS Chemical Economics Handbook – Toluene*, 2016.
141 E. Linak, A. Kishi, M. Guan and U. Buchholz, *IHS Chemical Chemical Economics Handbook – Furfural*, 2016.
142 S. K. Green, *et al.*, Diels–Alder cycloaddition of 2-methylfuran and ethylene for renewable toluene, *Appl. Catal., B*, 2016, **180**, 487–496.
143 Y.-T. Cheng and G. W. Huber, Production of targeted aromatics by using Diels–Alder classes of reactions with furans and olefins over ZSM-5, *Green Chem.*, 2012, **14**, 3114.
144 J. Lessard, J.-F. Morin, J.-F. Wehrung, D. Magnin and E. Chornet, High Yield Conversion of Residual Pentoses into Furfural via Zeolite Catalysis and Catalytic Hydrogenation of Furfural to 2-Methylfuran, *Top. Catal.*, 2010, **53**, 1231–1234.
145 A. Mandalika and T. Runge, Enabling integrated biorefineries through high-yield conversion of fractionated pentosans into furfural, *Green Chem.*, 2012, **14**, 3175–3184.
146 L. W. Burnett, I. B. Johns, R. F. Holdren and R. M. Hixon, Production of 2-Methylfuran by Vapor-Phase Hydrogenation of Furfural, *Ind. Eng. Chem.*, 1948, **40**, 502–505.
147 M. J. Gilkey, *et al.*, Mechanistic Insights into Metal Lewis Acid-Mediated Catalytic Transfer Hydrogenation of Furfural to 2-Methylfuran, *ACS Catal.*, 2015, **5**, 3988–3994.
148 W. Zhang, Y. Zhu, S. Niu and Y. Li, A study of furfural decarbonylation on K-doped Pd/Al2O3 catalysts, *J. Mol. Catal. A: Chem.*, 2011, **335**, 71–81.
149 L. Jiang, *et al.*, Enhanced propionic acid production from whey lactose with immobilized Propionibacterium acidipropionici and the role of trehalose synthesis in acid tolerance, *Green Chem.*, 2015, **17**, 250–259.

150 Z. Wang, Y. Jin and S.-T. Yang, High cell density propionic acid fermentation with an acid tolerant strain of Propionibacterium acidipropionici, *Biotechnol. Bioeng.*, 2015, **112**, 502–511.
151 M. Kitson and P. S. Williams, *Alcohols production by hydrogenation of carboxylic acids*, 1989.
152 H. Taheri, Y. Sarin and B. Ozero, *Process and reactor for dehydration of propanol to propylene*, 2015.
153 B. Erdei, *et al.*, Ethanol production from mixtures of wheat straw and wheat meal, *Biotechnol. Biofuels*, 2010, **3**, 16.
154 E. Varga, K. Réczey and G. Zacchi, Optimization of steam pretreatment of corn stover to enhance enzymatic digestibility, *Appl. Biochem. Biotechnol.*, 2004, **114**, 509–523.
155 A. Morschbacker, Bio-Ethanol Based Ethylene, *Polym. Rev.*, 2009, **49**, 79–84.
156 C. Eckert, *et al.*, Ethylene-forming enzyme and bioethylene production, *Biotechnol. Biofuels*, 2014, **7**, 33.
157 W. Xiong, *et al.*, The plasticity of cyanobacterial metabolism supports direct CO2 conversion to ethylene, *Nat. Plants*, 2015, **1**, 15053.
158 K. Smith, M. Pampel and P. Feng, *IHS Chemical Chemical Economics Handbook – Xylenes*, 2015.
159 J. A. Kent, *Riegel's Handbook of Industrial Chemistry*, Springer Science & Business Media, 2012.
160 Sulzer Chemtech, *Separation Technology for the Chemical Process Industry*, 2010.
161 Y. Román-Leshkov, C. J. Barrett, Z. Y. Liu and J. A. Dumesic, Production of dimethylfuran for liquid fuels from biomass-derived carbohydrates, *Nature*, 2007, **447**, 982–985.
162 C. V. Nguyen, *et al.*, Combined treatments for producing 5-hydroxymethylfurfural (HMF) from lignocellulosic biomass, *Catal. Today*, 2016, **278**(Part 2), 344–349.
163 L. Atanda, *et al.*, High yield conversion of cellulosic biomass into 5-hydroxymethylfurfural and a study of the reaction kinetics of cellulose to HMF conversion in a biphasic system, *Catal. Sci. Technol.*, 2016, **6**, 6257–6266.
164 H. Mirzaei and B. Karimi, Sulphanilic acid as a recyclable bifunctional organocatalyst in the selective conversion of lignocellulosic biomass to 5-HMF, *Green Chem.*, 2016, **18**, 2282–2286.
165 S. Nishimura, N. Ikeda and K. Ebitani, Selective hydrogenation of biomass-derived 5-hydroxymethylfurfural (HMF) to 2,5-dimethylfuran (DMF) under atmospheric hydrogen pressure over carbon supported PdAu bimetallic catalyst, *Catal. Today*, 2014, **232**, 89–98.
166 J. Carvajal-Diaz and D. Byrne, *IHS Chemical Chemical Economics Handbook – Ethylbenzene*, 2015.
167 J. Maul, *et al.*, in *Ullmann's Encyclopedia of Industrial Chemistry*, Wiley-VCH Verlag GmbH & Co. KGaA, 2000. DOI: 10.1002/14356007.a21_615.pub2.
168 J.-S. Chang, S.-E. Park, Q. Gao, G. Férey and A. K. Cheetham, Catalytic conversion of butadiene to ethylbenzene over the nanoporous nickel(II) phosphate, VSB-1, *Chem. Commun.*, 2001, 859–860, DOI: 10.1039/B009160J.
169 J. Q. Bond, D. M. Alonso, D. Wang, R. M. West and J. A. Dumesic, Integrated Catalytic Conversion of γ-Valerolactone to Liquid Alkenes for Transportation Fuels, *Science*, 2010, **327**, 1110–1114.
170 D. M. Alonso, J. M. R. Gallo, M. A. Mellmer, S. G. Wettstein and J. A. Dumesic, Direct conversion of cellulose to levulinic acid and gamma-valerolactone using solid acid catalysts, *Catal. Sci. Technol.*, 2013, **3**, 927–931.
171 M. D. Jones, Catalytic transformation of ethanol into 1,3-butadiene, *Chem. Cent. J.*, 2014, **8**, 53.
172 H. Yim, *et al.*, Metabolic engineering of *Escherichia coli* for direct production of 1,4-butanediol, *Nat. Chem. Biol.*, 2011, **7**, 445–452.
173 A. Burgard, M. J. Burk, R. Osterhout, S. Van Dien and H. Yim, Development of a commercial scale process for production of 1,4-butanediol from sugar, *Curr. Opin. Biotechnol.*, 2016, **42**, 118–125.
174 C. Ma, *et al.*, Enhanced 2,3-butanediol production by *Klebsiella pneumoniae* SDM, *Appl. Microbiol. Biotechnol.*, 2009, **82**, 49–57.
175 L. Zhang, *et al.*, Microbial production of 2,3-butanediol by a surfactant (serrawettin)-deficient mutant of *Serratia marcescens* H30, *J. Ind. Microbiol. Biotechnol.*, 2010, **37**, 857–862.
176 H. Duan, Y. Yamada and S. Sato, Efficient production of 1,3-butadiene in the catalytic dehydration of 2,3-butanediol, *Appl. Catal., A*, 2015, **491**, 163–169.
177 S. Bizzari, B. Sesto and S. Liu, *IHS Chemical Chemical Economics Handbook - Benzoic Acid*, 2014.
178 J. G. Hundley and F. Nathan, *Manufacture of benzoic acid from toluene*, 1965.
179 E. Mahmoud, J. Yu, R. J. Gorte and R. F. Lobo, Diels–Alder and Dehydration Reactions of Biomass-Derived Furan and Acrylic Acid for the Synthesis of Benzoic Acid, *ACS Catal.*, 2015, **5**, 6946–6955.
180 T. Salavati-fard, S. Caratzoulas, R. F. Lobo and D. J. Doren, Catalysis of the Diels–Alder Reaction of Furan and Methyl Acrylate in Lewis Acidic Zeolites, *ACS Catal.*, 2017, **7**, 2240–2246.
181 Y. Wang, *et al.*, Chemical synthesis of lactic acid from cellulose catalysed by lead(II) ions in water, *Nat. Commun.*, 2013, **4**, 1–7.
182 X. Zhang, L. Lin, T. Zhang, H. Liu and X. Zhang, Catalytic dehydration of lactic acid to acrylic acid over modified ZSM-5 catalysts, *Chem. Eng. J.*, 2016, **284**, 934–941.
183 X. Li and Y. Zhang, Oxidative Dehydration of Glycerol to Acrylic Acid over Vanadium-Substituted Cesium Salts of Keggin-Type Heteropolyacids, *ACS Catal.*, 2016, **6**, 2785–2791.
184 T. Gao, Y. Wong, C. Ng and K. Ho, L-lactic acid production by *Bacillus subtilis* MUR1, *Bioresour. Technol.*, 2012, **121**, 105–110.
185 V. Kumar, S. Ashok and S. Park, Recent advances in biological production of 3-hydroxypropionic acid, *Biotechnol. Adv.*, 2013, **31**, 945–961.

186 K. Smith, *IHS Chemical Chemical Economics Handbook - Phthalic Anhydride*, 2015.
187 N. Alonso-Fagúndez, M. L. Granados, R. Mariscal and M. Ojeda, Selective Conversion of Furfural to Maleic Anhydride and Furan with VOx/Al2O3 Catalysts, *ChemSusChem*, 2012, **5**, 1984–1990.
188 J. J. Bozell, *et al.*, Production of levulinic acid and use as a platform chemical for derived products, *Resour., Conserv. Recycl.*, 2000, **28**, 227–239.
189 K. Smith, P. Sriram and A. Pujari, *IHS Chemical Chemical Economics Handbook - Dimethyl Terephthalate (DMT) and Terephthalic Acid (TPA)*, 2013.
190 K. K. Miller, P. Zhang, Y. Nishizawa-Brennen and J. W. Frost, Synthesis of Biobased Terephthalic Acid from Cycloaddition of Isoprene with Acrylic Acid, *ACS Sustainable Chem. Eng.*, 2014, **2**, 2053–2056.
191 O. Casanova, S. Iborra and A. Corma, Biomass into Chemicals: Aerobic Oxidation of 5-Hydroxymethyl-2-furfural into 2,5-Furandicarboxylic Acid with Gold Nanoparticle Catalysts, *ChemSusChem*, 2009, **2**, 1138–1144.
192 S. Mizuno, N. Yoshikawa, M. Seki, T. Mikawa and Y. Imada, Microbial production of *cis, cis*-muconic acid from benzoic acid, *Appl. Microbiol. Biotechnol.*, 1988, **28**, 20–25.
193 D. R. Vardon, *et al.*, Adipic acid production from lignin, *Energy Environ. Sci.*, 2015, **8**, 617–628.
194 C. W. Johnson, *et al.*, Enhancing muconic acid production from glucose and lignin-derived aromatic compounds via increased protocatechuate decarboxylase activity, *Metab. Eng. Commun.*, 2016, **3**, 111–119.
195 J. W. Frost, A. Miermont, D. Schweitzer and V. Bui, *Preparation of trans, trans muconic acid and trans, trans muconates*, 2013.
196 F. Héroguel, B. Rozmysłowicz and J. S. Luterbacher, Improving Heterogeneous Catalyst Stability for Liquid-phase Biomass Conversion and Reforming, *Chim. Int. J. Chem.*, 2015, **69**, 582–591.
197 P. F. H. Harmsen, M. M. Hackmann and H. L. Bos, Green building blocks for bio-based plastics, *Biofuels, Bioprod. Biorefin.*, 2014, **8**, 306–324.
198 D. Cespi, F. Passarini, I. Vassura and F. Cavani, Butadiene from biomass, a life cycle perspective to address sustainability in the chemical industry, *Green Chem.*, 2016, **18**, 1625–1638.
199 Z. Lin, V. Nikolakis and M. Ierapetritou, Life Cycle Assessment of Biobased p-Xylene Production, *Ind. Eng. Chem. Res.*, 2015, **54**, 2366–2378.
200 Z. Lin, V. Nikolakis and M. Ierapetritou, Alternative Approaches for p-Xylene Production from Starch: Techno-Economic Analysis, *Ind. Eng. Chem. Res.*, 2014, **53**, 10688–10699.
201 Z. Lin, M. Ierapetritou and V. Nikolakis, Aromatics from Lignocellulosic Biomass: Economic Analysis of the Production of p-Xylene from 5-Hydroxymethylfurfural, *AIChE J.*, 2013, **59**, 2079–2087.
202 G. Fiorentino, M. Ripa and S. Ulgiati, Chemicals from biomass: technological versus environmental feasibility. A review, *Biofuels, Bioprod. Biorefin.*, 2017, **11**, 195–214.
203 B. J. Nikolau, M. A. D. N. Perera, L. Brachova and B. Shanks, Platform biochemicals for a biorenewable chemical industry, *Plant J.*, 2008, **54**, 536–545.
204 N. Hadadi, J. Hafner, A. Shajkofci, A. Zisaki and V. Hatzimanikatis, ATLAS of Biochemistry: A Repository of All Possible Biochemical Reactions for Synthetic Biology and Metabolic Engineering Studies, *ACS Synth. Biol.*, 2016, **5**, 1155–1166.
205 N. Hadadi and V. Hatzimanikatis, Design of computational retrobiosynthesis tools for the design of de novo synthetic pathways, *Curr. Opin. Chem. Biol.*, 2015, **28**, 99–104.
206 M. H. Wagner, *et al.*, The strain-hardening behaviour of linear and long-chain-branched polyolefin melts in extensional flows, *Rheol. Acta*, 2000, **39**, 97–109.
207 S. Corneillie and M. Smet, PLA architectures: the role of branching, *Polym. Chem.*, 2015, **6**, 850–867.
208 K. Okura, *et al.*, Synthesis of Polysubstituted Benzenes from 2-Pyrone-4,6-dicarboxylic Acid, *Chem. Lett.*, 2014, **43**, 1349–1351.
209 J. H. Gibbs and E. A. DiMarzio, Nature of the Glass Transition and the Glassy State, *J. Chem. Phys.*, 1958, **28**, 373–383.
210 A. H. Willbourn, The glass transition in polymers with the (CH 2) n group, *Trans. Faraday Soc.*, 1958, **54**, 717–729.
211 P. C. Hiemenz and T. P. Lodge, *Polymer Chemistry*, CRC Press, 2nd edn, 2007.
212 Plastic News, Current Resin Pricing, *Plastic News*, 2017. available at: http://www.plasticsnews.com/resin/thermosets/current-pricing (accessed: 8th March 2017).
213 A. Corma, Attempts to Fill the Gap Between Enzymatic, Homogeneous, and Heterogeneous Catalysis, *Catal. Rev.*, 2004, **46**, 369–417.

